https://doi.org/10.1016/j.rser.2021.111082

Research Development of Indirect Evaporative Cooling Technology: an Updated Review

Hongxing Yang [a, *], Wenchao Shi [a, *], Yi Chen [b], Yunran Min [a]

[a] Renewable Energy Research Group (RERG), Department of Building Services Engineering, The Hong Kong Polytechnic University, Hong Kong, China
[b] Division of Science, Engineering and Health Studies, College of Professional and Continuing Education (CPCE), The Hong Kong Polytechnic University, Hong Kong, China

Abstract

Driven by the economic outbreak and the growing demand of thermal comfort, the energy consumption of air conditioning (AC) keeps increasing promptly. Indirect evaporative cooling, as an energy-efficient and eco-friendly AC approach, attracts attention in recent years. However, this traditional technology has some drawbacks associated with its working principles. For instance, the limited output temperature constrains its application scopes. Insufficient evaporation due to the poor wettability on the wet channel surface significantly affects the cooling performance. This study provides an updated review of the research progress for solving these problems. Specifically, lower-temperature air can be produced by dew-point evaporative coolers. Innovative wicks with different materials strengthen the surface wettability as well as promote evaporation. Besides, hybrid systems and system optimizations can ensure cooling performance under hot-arid and hot-humid weather conditions. With the recent developments and foreseeable future opportunities to cope with these problems, IEC is expected to make more contributions to reducing the energy consumption of AC in buildings.

Highlight:

- Performance enhancement approaches for indirect evaporative cooling are reviewed.
- The applications of indirect evaporative cooling in hot-dry and hot-humid regions are analyzed.
- Materials for indirect evaporative coolers are summarized.
- Hybrid systems and system optimizations are discussed.

Keywords:

Indirect evaporative cooling
Performance enhancement
Material
Hybrid system
Optimization

(Word count: 11182)

Nomenclature

A_{ratio}	ratio of heat transfer area to primary air flow volume, $m^2/(m^3/s)$	*ew*	Evaporation water
c_{pa}	specific heat of air, J/(kg·℃)	*in*	inlet air
c_{pw}	specific heat of water, J/(kg·℃)	*out*	outlet air
d	channel gap, m	*p*	primary air channel
d_e	hydraulic diameter of channel, m	*s*	secondary air channel
g	acceleration of gravity, m/s^2	*w*	water film
H	height of cooler, m	*wb*	wet-bulb
h	heat transfer coefficient, $W/(m^2 \cdot ℃)$		
h_{fg}	latent heat of vaporization of water, J/kg		
h_m	mass transfer coefficient, kg/ $(m^2 \cdot s)$	*Abbreviation*	
i	enthalpy, kJ/kg	1/2/3-D	one/two/three dimensional
L	length of cooler, m	AC	air conditioning
m	mass flow rate of air, kg/s	AHU	air handling unit

* corresponding author
Email addresses: hong-xing.yang@polyu.edu.hk (H. Yang); wenchao511.shi@connect.polyu.hk (W. Shi)

m_{ratio}	ratio of primary to secondary air flow volume	CCU	cooling coil unit
Pr	Prandtl number	CFD	computational fluid dynamics
R_{con}	condensation ratio	COP	coefficient of performance
Re	Reynolds number	DEC	direct evaporative cooling
Sh	Sherwood number	DPIEC	dew point indirect evaporative cooler
St	Stanton number	DS	dimension size
t	Temperature, ℃	DW	desiccant wheel
u	air velocity, m/s	DWC	dropwise condensation
V	air flow volume, m^3/s	EC	Evaporative cooling
		FDM	finite difference method
Greek symbols		FWC	filmwise condensation
ω	moisture content of air, g/kg	GHE	ground heat exchanger
δ	thickness, mm	INC	inlet conditions
θ	dimensionless temperature	LDD	liquid desiccant dehumidifier
φ	relative humidity, %	RC	radiative cooling
λ	thermal conductivity W/(m·℃)	NTU	number of transfer unit
ρ	density, kg/m^3	NRC	nocturnal radiative cooling
μ	dynamic viscosity, Pa·s	PC	passive cooling
υ	kinematic viscosity, m^2/s	PUA	packaged unit of air conditioner
η	effectiveness	RH	relative humidity
ε_{en}	enlargement coefficient	RIEC	regenerative indirect evaporative cooling
		SD	solid desiccant
Subscripts		S/P	secondary-to-primary air
c	cooling	VCRS	vapor compression refrigeration system
cw	condensation water	WBT	wet-bulb temperature
dew	dew point	W/I	working-to-intake air

1. Introduction

Living standard improvement results in more energy consumption on AC systems to satisfy thermal comfort requirements [1]. It has been reported that people spent almost 90% of time in air-conditioned space, which led to continuous consumption of natural resources for creating an artificial built environment [2]. In China, the energy demand for cooling in buildings proliferated with climate change and users' greater affordability over the past two decades. It increased by 13% every year from 2000, and the total electricity usage reached about 400 TWh in 2017, which consequently caused fivefold cooling-related CO2 emissions from electricity consumption [3, 4]. Thus, it is crucial to develop novel approaches for reducing the energy consumption of AC systems as well as guaranteeing thermal comfort and indoor air quality [5].

It is estimated by International Energy Agency (IEA) that the efficient cooling scenario can almost halve energy consumption for AC, reducing investment and operating costs by 3 trillion US dollars between now and 2050 [6]. Indirect evaporative cooling, which removes heat through the evaporation process, has been regarded as one of the promising solutions to substitute conventional AC, especially in desert and semi-arid regions [7-9]. What's more, it has started to be applied under hot and humid climatic conditions for the fresh air pre-cooling [10]. Compared with vapor compression refrigeration, the benefits of this technology are worthy of being stressed because it does not employ compressors and environmental-harmful chemical refrigerants. In the past few decades, plenty of studies have been conducted on indirect evaporative cooler (IEC) to evaluate the feasibility, improve the thermal performance, and expand its application regions [11-13]. For instance, the DPIEC was proposed based on simple plate-type IEC to acquire lower outlet temperature of product air [14]. Different materials were embedded or fabricated to the IEC to enhance the heat and mass transfer process [15-17]. In addition, hybrid IEC systems were employed to develop their energy-saving potential in hot-humid areas when the evaporation rate of traditional IEC is not as intense as it in dry regions [18].

Nowadays, IEC has been closely relevant to plenty of fields. As a passive cooling device, it could be responsible for cooling production, energy recovery, and ventilation in buildings [10, 19, 20]. With proper modification and combination, water desalination was also achieved by IEC [21]. Besides, it has

been revealed to use IEC for some agricultural storage issues [22]. The review focus of some recently published papers is provided in Table 1. It can be identified that IEC was frequently taken as a branch to be elaborated under a general topic of evaporative cooling, which was normally illustrated with DEC rather than being reviewed in an individual paper. In addition to generally sketching the working principles and hybrid systems, the essential equations and correlations, internal structures and enhanced materials, optimizations of the water spraying system of IEC, which has seldomly been summarized in the existing literature, were discussed.

In order to systematically review the recent progress on IEC technology, this paper is divided into three sections. In the first part, several configurations of IEC are introduced with the critical heat and mass transfer equations. The second part is devoted to the studies on accessible materials selected for manufacturing the IEC and their impact on cooling effects. Different types of hybrid IEC systems and related optimization are illustrated in the last section.

Table 1. Comparison among previous and present review works

Study	Country/ Region	General focus	Detailed focus
[23, 24]	China	EC	Hybrid systems and equipment of DEC and IEC.
[25]	India	PC	System configurations and optimizations of DEC, IEC, NRC, and phase change materials.
[26]	Worldwide	M-cycle	Working principle and hybrid systems
[27]	Hot and humid regions	LD/EC	Principle operation and hybrid systems combined dehumidification device with DEC or IEC.
[28]	Worldwide	EC	Enhancement of DEC or IEC by integrating various desiccant dehumidification sections.
[29]	Worldwide	EC	Working principle, building application, performance assessment, and techno-economical and environmental analysis of DEC and IEC
Present study	Worldwide	IEC	Working principle, essential equations and correlations, materials, novel internal structures, hybrid system, water spraying systems, and corresponding optimization.

2. The classifications of IECs

IECs can be mainly classified into the counter-flow type and cross-flow type according to the airstream directions (Fig. 1). Besides, tubular type and other configurations have also been studied. In an IEC unit, every two adjacent channels divided by thin plates are dry channel and wet channel, which are responsible for accommodating primary (product) air and secondary (working) air, respectively. Water is delivered by a pump and evenly sprayed on the wet vertical channels to generate a thin water film covering the plate surfaces. Due to the moisture content difference between the film and mainstream of the secondary air, continuous evaporation occurs to cool the plate. In the dry channel, the primary air is cooled by the plate through convective heat transfer without contacting the liquid water. Thus, no moisture content is added to the primary airstream. Recent studies on different kinds of IECs are presented in the following sub-sections.

(a) (b)

Fig. 1 Schematic diagram of (a) counter-flow IEC (b) cross-flow IEC [30]

2.1 Counter-flow IEC

As shown in Fig. 1(a), the air flows oppositely in the adjacent channels. It is known that the cooling limit temperature of primary air is the wet-bulb temperature (WBT) of the inlet secondary air. When the outdoor temperature is high, the output primary air temperature cannot satisfy the thermal comfort requirements due to the high WBT [31]. Intended for obtaining lower outlet temperature, two types of dew point indirect evaporative cooler (DPIEC), namely, Maisotsenko-cycle (M-cycle) cooler and regenerative indirect evaporative cooler (RIEC), have been proposed (Fig. 2). The M-cycle cooler introduces part of the cooled air from the dry channel while RIEC uses the air from the dry channel or the exhaust air from indoor air-conditioned spaces. Studies related to counter-flow IEC are summarized in Table 2.

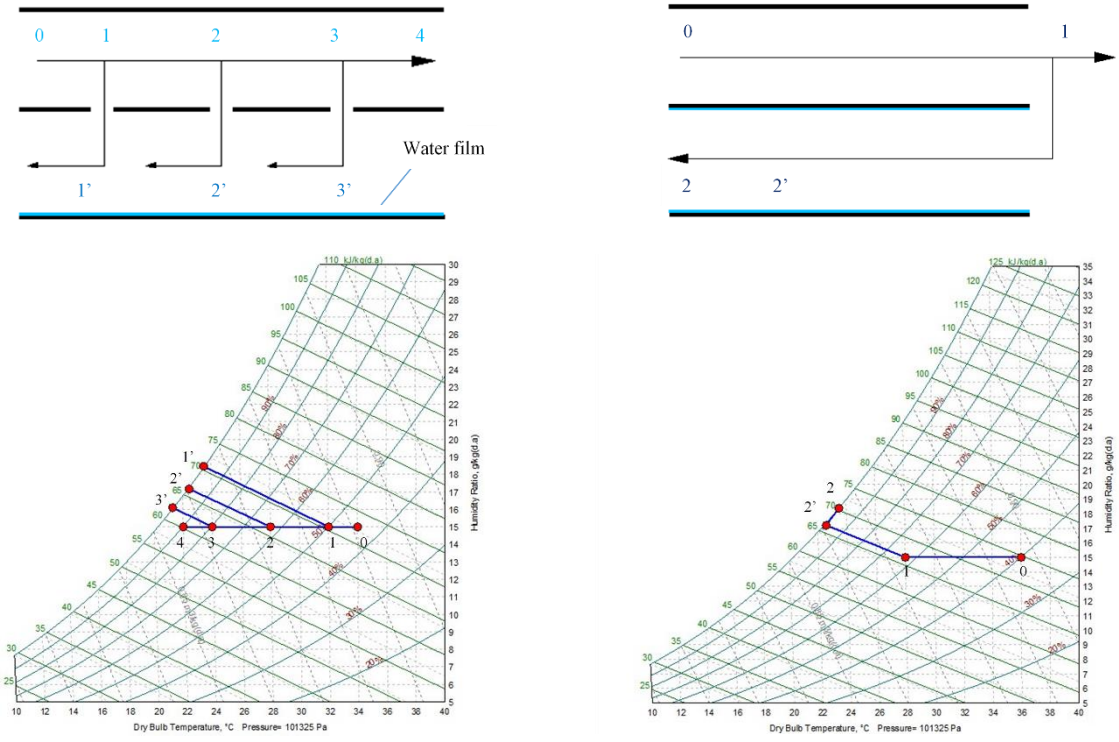

(a) (b)

Fig. 2 Working principle and psychrometric chart of (a) M-cycle cooler (b) RIEC

Table 2 Previous work on counter-flow-based IEC

Research	Geometric size of cooler			Inlet air condition			Features
	L (m)	W (m)	d (mm)	t (℃)	ω (g/kg dry air)/ RH (%)	u (m/s; m^3/h)	
Counter-flow [31]	0.1-2	-	2-10	t_p=24~40; t_s=20~28	ω_p= 30~90%; ω_s= 40~70%	0.5-5	1-D model was built for simulation considering condensation in the primary air passages when IEC was used in hot and humid regions. Enlargement coefficient and condensation area ratio were proposed to supplement the existing evaluation indices.
M-cycle [31, 32]	0.12	0.08	2	24.37-46.86	6.91-66.12%	2.4	W/I air ratio: 0.33. The probability of applying M-cycle cooler in Arab Gulf cities was checked. It was pointed out that the supply air of this device might not meet the comfort zone, but it would be more efficient for the same cooling production.
M-cycle [33]	0.9	0.04	4	25-45	12.7-18	0.88-1.5	W/I air ratio: 0.35~0.65. The aluminum surface in the wet passage was coated with Kraft paper to improve the surface wettability. M-cycle cooler augments the wet-bulb effectiveness at the cost of cooling capacity. The wet-bulb effectiveness exceeds 100% under each test condition.
M-cycle [34]	0.6-1.4	0.8	5	30	10	2	The IECs with the configurations of single purge and four purges on the channel surface were investigated. Single purge IEC produced more 20% cooling than four purges cooler and achieved higher effectiveness.
M-cycle [35]	0.2-1.5	0.5	2-10	30	40%	3	The ε-NTU model was proposed and validated by experimental data in the literature. The triangle channel was regarded to be the most effective, but it may suffer from poor water distribution.
Regenerative [8]	0.1-3	0.08	1-10	25-45	7-26	1.5-6	W/I air ratio: 0.05~0.95. The 1-D simulation model was developed and tested by a set of input air conditions. IEC design parameters such as air velocity, W/I air ratio, and geometrical sizes were optimized.
Regenerative [36]	0.5-1.2	0.18	2-6	27.5–40.0	8.0–18.0	1.0–3.0	W/I air ratio: 0.1–0.9. A 2-D mathematical model was established, and the product air temperature was derived by using dimensionless numbers or groups. The average heat and mass transfer coefficients ranged between 26.8 to 29.9 W/(m^2·K) and 0.025 to 0.027 kg/ (m^2 ·s), respectively.
Regenerative [37]	0.75	0.3	d_p=6; d_s=10	tp=27-37; ts=24	ω_p= 70~90%; ω_s= 60%	1.5-3	The return air from air-conditioned spaces was taken as secondary air. IEC pre-cooled the air and fulfilled 32% of the cooling load for an AHU under tropic weather conditions.
Regenerative [38]	0.9	0.314	6	24.9-36.4	17.1%-58.2%	-	Four types of wicking materials were bonded on the aluminum sheet to enhance the water absorption capacity. The tested RIEC was predicted to save 15% to 58% energy annually under various climate zones in China.
Regenerative [39]	-	-	-	t_p=35-38; t_s=25	ω_p= 65~70%; ω_s= 35, 50, 65%	54-90	IEC, with the enthalpy recovery from indoor return air, served for building ventilation in the hot-humid area. RIEC achieved higher enthalpy recovery efficiency than the existing rotary heat exchanger.
Regenerative [40]	0.9	0.314	6	22.7-38.9	9.3-19.4	1.58~ 2.83	W/I air ratio: 0.1–0.7. The spraying water temperature had less influence on the output parameters. The lower inlet air velocity and higher W/I air ratio benefit the effectiveness, whereas shrank the cooling capacity of IEC.
Regenerative [41]	0.6	0.15	5	t_p=30-35;	ω_p= 40-55%;	1-2	W/I air ratio: 0.2–0.7. The novel working-dry channel was designed to obtain lower wet-bulb temperature in the adjacent working air channel. Pre-cooling, energy recovery, and dehumidification were achieved at the same time.
Regenerative [42]	0.6	0.15	4.5	30.54-31.49	46-61%	0.98-2.14	W/I air ratio:0.45-0.69. The influences of counter and parallel working air directions with downside flowing water film on product air temperature were analyzed with experimental validation.
Regenerative [43]	0-4	0.32	1-12	33	35%	0.4-4	W/I air ratio:0.1-0.9. A novel model combined with energy relationship and the irreversible thermodynamic theory was developed. The entropy production number was found as a potential indicator for optimization purposes.

Note: p: primary air channel s: secondary air channel

2.1.1 Model establishment for condensation and non-condensation state

As shown in Table 2, research attentions were mainly taken to the impact of inlet air conditions and geometrical factors on effectiveness and COP. Among the models in summarized studies, some assumptions and equations are necessary for theoretical analysis, which should be stressed as follows [8].

1) The properties of water film and air were regarded to be steady and uniform in two channels.
2) IEC has no heat and mass exchange with its surroundings. Both heat and mass were only transferred along the flow direction of the fluid.
3) The thin water film entirely and evenly covered the surface of the wet channel.
4) The thermal conductivity of the plate and water film between the dry and wet sides was ignored because of the thin thickness.
5) Lewis number was considered to be constant.

The governing equations for counter-flow IEC describe the temperature and moisture content change as well as energy balance between the two channels. In the wet channel, the energy equation of the secondary air is written in Eq. (1).

$$m_s i_s = h_s(t_w - t_s)L \cdot dx + h_{fg} h_{ms}(\omega_{t_w} - \omega_s)L \cdot dx \tag{1}$$

For air-water vapor mixtures in the wet channel, Lewis number, a dimensionless number that bridges the relationship between heat and mass transfer coefficients, could be expressed by Eq. (2). In the evaporation process of water film in the wet channel and the condensation process in the dry channel, the value of Lewis number was set as 1 [44]. This value was also determined as 0.87 at standard atmospheric conditions in some research [7, 45, 46].

$$Le^{\frac{2}{3}} = \frac{h_s}{h_{ms} c_{pa}} \tag{2}$$

Besides, these two coefficients can be calculated through Nusselt number and Sherwood number, which has been presented in section 2.5, Table 5.

The energy balance equation of two channels is formulated by Eq. (3):

$$m_s i_s - m_p c_{pa} dt_p = d(c_{pw} t_{ew} m_e) \tag{3}$$

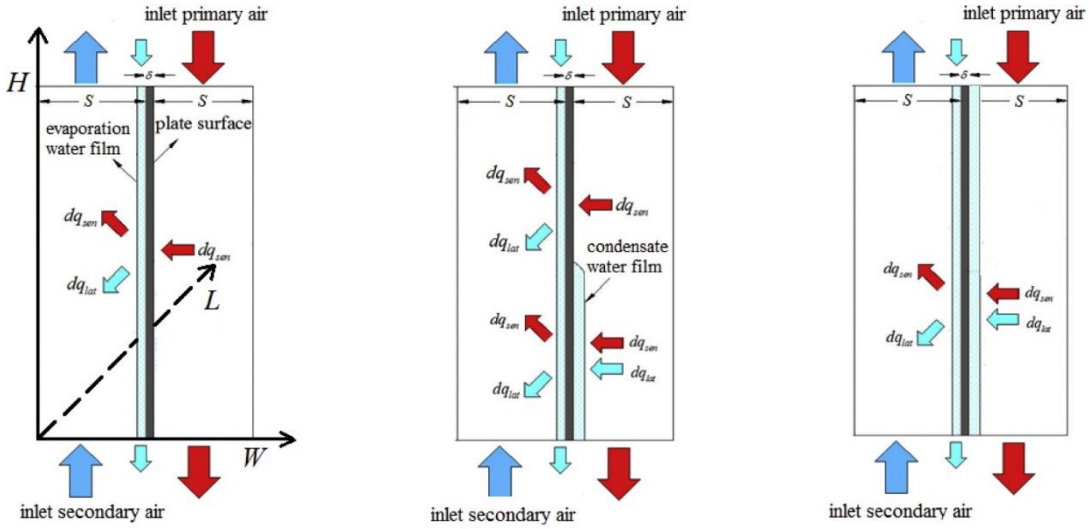

(a) Non-condensation state (b) Partial condensation state (c) Total condensation state

Fig. 3 Three condensation states of IEC [47]

It should be noticed that the above equations only describe the heat and mass transfer process of IEC in hot and arid regions because the outdoor air is dry enough and less likely to occur condensed water in the dry channel even though it is cooled to a low temperature. Nonetheless, the condensation may take place if the outdoor air is hot and humid, such as the summer weather condition in Hong Kong.

It occurs when the plate temperature is lower than the dew point temperature of the flowing air. As depicted in Fig. 3, referring to the condensation position in the channel, the status could be categorized into non-condensation state, partial condensation state, and total condensation state. In order to investigate the cooling effect in these three states, the moisture content balance equation for the dry channel should be supplemented (Eq. (4)), and the total energy balance equation also needs to be modified as Eq. (5) [47]:

$$h_{mp}(\omega_p - \omega_{t_w}) = m_p d\omega_p \tag{4}$$

$$m_s di_s - m_p di_p = d(c_{pw} t_{ew} m_{e)}) + d(c_{pw} t_{cw} m_c) \tag{5}$$

The finite difference method (FDM) was frequently used to discretize differential energy equations [8, 48]. All derivate terms of the governing equations were substituted by the discrete equivalents. After determining the boundary conditions, each element's temperature and moisture content can be quantified simultaneously by solving all the discrete equations. Computer software such as MATLAB was utilized to achieve the aforementioned process [34, 49].

With the vast improvement of computer power, the computational fluid dynamics (CFD) model was developed to couple the heat and mass transfer processes between the water and air, which relied on continuity, momentum, energy, and species equations [50]. CFD simulation can cope with complex hydraulic and thermal processes. Compared with programming the code to address complicated differential equations, the CFD approach is more simple and can consider multiple factors at the same time. Studies using CFD for parameter analysis are listed in Table 3. It was noted that the thickness of the water film was required for setting the boundary conditions and interfacial matching conditions in the model, which could be calculated by the empirical formula as follows [41, 51]:

$$\delta = \left(\frac{3\mu_w m_w}{{\rho_w}^2 g}\right)^{\frac{1}{3}} \tag{6}$$

Table 3 IEC studies with CFD approach

Research	Software	Features
[52]	Ansys fluent	The influences of channel size, physical ribs along the channel, and using return air as secondary air on a DPIEC were discussed.
[53]	Ansys fluent	The average Nusselt number for the dry and wet channels and Sherwood number for the wet channel were analyzed. Nusselt number and Sherwood number were expressed by several dimensionless factors.
[54]	Ansys fluent	IEC that removed supporting guides was simulated in CFD environment. The efficiency of this irregular cooler was significantly higher than the normal one, making it possible to shrink the IEC size and initial cost.
[55]	Ansys fluent	Lower air velocity, smaller channel height, and lower S/P air ratio were proved that would lead to greater efficiency.
[56]	COMSOL	Empirical equations of heat and mass transfer coefficient were formulated by several inlet air parameters under tropical climatic conditions.
[57]	Ansys fluent	IEC with energy recovery from the cool indoor air was examined. Given the local weather conditions, this model could predict the condensation effects.
[58]	Ansys fluent	A three-dimensional model was developed. The air temperature, velocity, and vapor concentration distribution in the cooler were worked out. The pressure gradient was analyzed with the change of the channel gap distance.

2.1.2 Evaluation indices

The wet-bulb and dew point effectiveness, cooling capacity, and COP are considered to assess the performance of the IEC. Wet-bulb and dew point effectiveness were frequently used (Eq. (7) - (8)) [30, 59, 60], which are defined by the ratio of the inlet and outlet primary air temperature difference to the difference between primary air and web-bulb/dew point temperature of inlet secondary air, respectively, reflecting the ability to handle sensible heat [61]. For an IEC system, the cooling capacity depends on

the air flowrate and the difference of inlet and outlet primary air temperature (Eq. (9)). To maintain the fluid distribution and system operation, the pumps and fans consume electrical power. The coefficient of performance (COP) bridges the correlation between output cooling and input energy ((Eq. (10)).

$$\eta_{wb} = \frac{t_{p,in} - t_{p,out}}{t_{p,in} - t_{s,in,wb}} \tag{7}$$

$$\eta_{dp} = \frac{t_{p,in} - t_{p,out}}{t_{p,in} - t_{s,in,dew}} \tag{8}$$

$$Q_c = m_p c_{pa}(t_{p,in} - t_{p,out}) \tag{9}$$

$$COP = \frac{Q_c}{W} \tag{10}$$

When the ambient air is hot and humid, the air cooling and dehumidification process happens simultaneously in the primary air passage. However, wet-bulb and dew point effectiveness cannot evaluate the total heat transfer process. Therefore, enthalpy effectiveness and enlargement coefficient are mentioned. Enthalpy effectiveness is defined by the ratio of the enthalpy difference between inlet and outlet air in the dry channel to the enthalpy difference between primary inlet air and secondary inlet air (Eq. (11)) [62, 63]. The enlargement coefficient is the degree of enlarged heat exchanger rate due to the condensation, given by Eq. (12) [31, 60].

$$\eta_{enthaply} = \frac{i_{p,in} - i_{p,out}}{i_{p,in} - i_{s,in}} \tag{11}$$

$$\varepsilon_{en} = \frac{Q_{total}}{Q_{sensible}} \tag{12}$$

2.1.3 Correlation studies

Numerical studies are responsible for parametric analysis and optimization, which usually experience a complicated process for a long time. When IEC is utilized in engineering, workers need to design the system properly in a short period. Thus, the correlation study is crucial since it can provide a more straightforward approach to calculate results within an acceptable discrepancy. The work efficiency can be improved due to the simple calculation procedure. Combined with building simulation software such as TRNSYS, the annual performance of IEC could be predicted. What's more, referring to the correlation equation, it is clear to identify the relative importance of each factor [64]. For example, Pakari and Ghani developed a regression model for a counter-flow DPIEC. The outlet air state was formulated by inlet operational parameters and geometric sizes. The obtained correlation equations for outlet air matched the numerical and experimental data within only 4% and 10% discrepancy, respectively. According to Wan et al., the correlations of heat and mass transfer coefficients (Eq. (13)-(16)) and outlet temperature (Eq. (17)) were developed for a counter-flow IEC [14, 56]. It was summarized from the correlation formulas that the gap distance of channels was most influential to the convective heat transfer coefficients of primary air and secondary air and the mass transfer coefficient in the wet channel. Re_p had the most significant impact on the primary outlet dimensionless temperature $\theta_{p,o}$ than other four indices.

$$h_p = 134.684 t_{p,in}^{0.014} \varphi_{p,in}^{0.023} u_{p,in}^{0.014} L^{-0.048} d^{-1.001} \tag{13}$$

$$h_s = 85.155 t_{p,in}^{-0.164} \varphi_{p,in}^{-0.141} t_{s,in}^{0.327} d^{-1.176} \tag{14}$$

$$h_{mp} = 498.132 t_{p,in}^{-0.727} \varphi_{p,in}^{-0.95} u_{p,in}^{0.112} t_{s,in}^{0.441} \varphi_{s,in}^{0.164} d^{-0.8} \tag{15}$$

$$h_{ms} = 132.139 t_{p,in}^{0.127} \varphi_{s,in}^{0.14} H^{-1.243} \tag{16}$$

$$\theta_{p,o} = 0.207 \alpha_L^{-0.157} R_{ws}^{0.089} Re_p^{0.296} \theta_{s,in}^{0.012} \theta_{w,in}^{0.04} \tag{17}$$

Zhu et al. identified influential dimensionless parameters and worked out a correlation for evaluating the dew point effectiveness of M-cycle coolers in 2.35% and 6.75% mean absolute deviations compared with numerical results and experimental data, respectively [65]. The correlation was written as:

$$\eta_{dew} = 5.79 St_p^{0.54} (St_{sd} St_{sw})^{-0.11} DS^{0.45} {INC_1}^{-0.32} {INC_2}^{0.22} \quad (18)$$

2.2 Cross-flow IEC

2.2.1 Model establishment for condensation and non-condensation state

In Fig. 1(b), the two air streams are orthogonal in separated channels without direct contact. As the air streams flow in two directions, the 1-D model cannot satisfy research purposes, which promote the establishment of the 2-D model. Previous works of cross-flow IEC are outlined in Table 4. One early research by Guo and Zhao has numerically investigated the cross-flow IEC [48]. The influences of inlet air conditions, geometric index, and surface wettability of the plate were discussed. Recently, a numerical study on a comprehensive comparison of counter- and cross-flow IEC was carried out [30]. These two research illustrated the equations commonly used to describe the 2-D heat and mass transfer process. The assumptions described in section 2.1.1 are still adopted for the following formulas.

In the wet channel, the heat and mass transfer between water film and secondary air can be expressed as follows:

$$h_s(t_w - t_s) \cdot dxdy + h_{fg} h_{ms} (\omega_{t_w} - \omega_s) dxdy = m_s \frac{\partial i_s}{\partial y} dy \quad (19)$$

The total heat exchange equation of two channels is written as:

$$m_s \frac{\partial i_s}{\partial y} - c_{pa} m_p \frac{\partial t_p}{\partial x} = c_{pw} t_{ew} \frac{\partial m_e}{\partial y} \quad (20)$$

The cross-flow IEC is applicable in hot and humid regions, playing as not only an air cooling device but a dehumidifier if the secondary air is from the cool indoor space. Thus, it is essential to develop a mathematical model considering the condensation state. Analogous to the method used for counter-flow IEC, the humidity balance equation between primary air and condensed water on the dry channel surface is supplemented by Eq. (21). Accordingly, the total energy balance equation is revised into Eq. (22):

$$h_{mp} (\omega_p - \omega_{t_w}) \cdot dxdy = m_p \frac{\partial \omega_p}{\partial x} \cdot dx \quad (21)$$

$$m_s \frac{\partial i_s}{\partial y} - m_p \frac{\partial i_p}{\partial x} = \frac{\partial (c_{pw} m_e t_{ew})}{\partial y} + \frac{\partial (c_{pw} m_c t_{cw})}{\partial x} \quad (22)$$

The above differential governing equations are discretized by the FDM to algebraic equations. By combining boundary conditions, the values of parameters in each element can be figured out.

It can be observed from Table 4 that the research focus of cross-flow IEC is similar to it of counter-flow IEC, surveying effects of the inlet air condition, the geometrical factors, and the source of secondary air. The cross-flow type is more available on a daily basis due to the easier airflow arrangement and smaller volume, but the effectiveness is lower than the counter-flow type in the same physical size by 7% and 2-3% on average for non-condensation and condensation state, respectively [30].

2.2.2 Evaluation indices

The evaluation indices for cross-flow IEC under condensation and non-condensation states are the same as counter-flow IEC, which can be found in section 2.1.2.

2.2.3 Correlation studies

In order to facilitate the application in engineering, efforts were also made on the correlation study of cross-flow IEC. Min et al. developed a simplified approach to predicting IEC's performance in the engineering stage [60]. The wet-bulb effectiveness of IEC under condensation and non-condensation state was expressed as functions of several inlet air parameters with coefficients (Eq. (23)-(24)), which could avoid the complicated simulation process so that engineers' work efficiency would be improved. The simplified functions could predict the wet-bulb effectiveness within the discrepancy of 9.5% and 4.3% for non-condensation states and condensation states compared with the experimental data.

$$\begin{aligned}\eta_{wb,NC} = {} & 0.682 + 0.0031t_{p,\,\mathrm{in}} - 0.0087RH_{p,\,\mathrm{in}} + 0.0058t_{s,\,\mathrm{in}} + 0.0141RH_{s,\,\mathrm{in}} - 0.1375V_p \\ & -0.2608m_{\mathrm{ratio}} + 0.0012A_{\mathrm{ratio}} - 0.0001t_{p,\,\mathrm{in}}\,t_{s,\,\mathrm{in}} + 0.0011t_{p,\,\mathrm{in}}\,m_{\mathrm{ratio}} \\ & +0.0428RH_{s,\,\mathrm{in}}\,m_{\mathrm{ratio}} + 0.0004V_pA_{\mathrm{ratio}} - 0.0002V_pm_{\mathrm{ratio}}\,A_{\mathrm{ratio}}\end{aligned} \quad (23)$$

$$\begin{aligned}\eta_{wb,C} = {} & -0.044 + 0.023t_{p,\,\mathrm{in}} + 0.729RH_{p,\,\mathrm{in}} + 0.0439t_{s,\,\mathrm{in}} + 0.4399RH_{s,\,\mathrm{in}} - 0.1072V_p \\ & -0.1021m_{\mathrm{ratio}} + 0.0009A_{\mathrm{ratio}} - 0.0009t_{p,\,\mathrm{in}}\,t_{s,\,\mathrm{in}} - 0.0156t_{p,\,\mathrm{in}}\,RH_{s,\,\mathrm{in}} - 0.0266RH_{p,\,\mathrm{in}}\,t_{s,\,\mathrm{in}} \\ & -0.4706RH_{p,\,\mathrm{in}}\,RH_{s,\,\mathrm{in}} - 0.352RH_{p,\,\mathrm{in}}\,m_{\mathrm{ratio}} + 0.0202RH_{s,\,\mathrm{in}} + 0.0054t_{s,\,\mathrm{in}}\,m_{\mathrm{ratio}}\end{aligned} \quad (24)$$

Table 4 Previous works on cross-flow-based IEC

Research	Geometry			Inlet air condition			Features
	L(m)	W(m)	d(mm)	t (℃)	ω (g/kg dry air)/ RH (%)	u/V (m/s; m^3/h)	
Cross-flow [66]	0.6	0.6	5	t_p=30-45; t_s=25-35	ω_p= 30% ω_s=10-50%	u_p=1-5; u_s=1-5	Effects of surface wettability factor and water membrane temperature were discussed. Experimental validation of the model considered the variable spraying water flow rate.
Cross-flow [15]	0.5	0.5	3.35	t_p=35; t_s=30-36.8	ω_p= 10; ω_s=10.6/13.6	u_p=3.7; u_s=3.7/5.7	With the significant impact of water flow rate, an IEC system was designed to cool the air as well as consume less water. The counter-flow configuration of nozzles and airflows led to a better cooling effect than parallel arrangement.
Cross-flow [30]	1	1	2-9	26-42	ω_p= 30-90%; ω_s= 40-70%	u_p =0.5-5; u_s=2	The proposed model could forecast the effect of condensed water in IEC under the weather conditions in some subtropical regions.
Cross-flow [48]	0.2	0.2	2-10	25-45	RH_s=10-90%	u_p=0.5~ 4.5;	Typical 2-D model for cross-flow IEC. The impacts of inlet air temperature, velocity, channel width, humidity were examined. Temperature and moisture content distributions were presented.
Cross-flow [67]	0.47	0.47	3.2	t_p=25/35; t_s=20~45	ω_p= 10; ω_s=6-14	u_p=3.7; u_s=3.7/5.7	Experiments using the operating air condition of the data center were carried out. The effects of secondary air parameters and surface wettability were discussed. The maximum temperature drop was 18℃ if the secondary air could be cold and dry.
Cross-flow [68]	0.7	0.7	7.2	t_p=20/35; t_s=20-30	ω_p=5; ω_s=5-13	V_p=1800; V_s=900-1800	Different sorts of protrusions were made on the plate surface. The corresponding pressure drop and wet-bulb effectiveness based on the particular geometry were analyzed.
M-cycle [69]	L_p=0.508 L_s=0.203	0.025	4	25-45	11.2-19	0.49-1.1	The wet channel surface made from aluminum was covered with felt to absorb more water. Experiments revealed that the temperature of sprayed water had few effects on effectiveness.
M-cycle [70]	0.5	0.23	3	t_p=30; t_s=24-26	ω_p= 37.5-45%; ω_s= 50-65%	3.5	Three kinds of airflow organizations were compared, namely, using the ambient air as the primary and secondary air, using the ambient air as the primary air and the air exhausted from the indoor AC area as the secondary air, using the mixture of the exhaust and ambient air as the primary and secondary air.
Regenerative [71]	1.2	0.08	0.02	25-48	0-15	V_p =864; V_s =260	The primary air of IEC was to offset the cooling load of human occupants. The output moist secondary air was delivered to the comfort zone of produce commodities so as to reduce the water consumption for humidification in desert or semi-arid regions.
Regenerative [49]	0.1-0.8	0.5	1-15	25-43	40%	0.5-6	W/I air ratio: 0.1~0.9. 2-D model for the regenerative cooler was built and validated by experiments. Wet-bulb effectiveness would reach 112% if inlet temperature, RH, and W/I air ratio were 30, 50% and 0.33, respectively.
Regenerative [72]	0.7	0.7	4.5	t_p=30; t_s=25	RH_p=45% RH_s=40-60%	500-800	The cool exhausted air was utilized as secondary air for heat recovery. This device could be used as an air cooler in summer and a heat recovery exchanger in winter based on experimental studies.

Note: p: primary air channel s: secondary air channel

2.3 Tubular IEC

An early experimental study by Tulsidasani et al. assessed the impact of air velocities on COP for a tube-type IEC. The outlet temperature, static pressure, and energy consumption were examined [73]. Recently, a prototype of the ceramics tubular IEC was manufactured (Fig. 4). For this cooler, water is sprayed on the outer surface of the ceramics pipe to generate water film. The fresh primary air flows inside the pipes horizontally, while the secondary air sweeps across the pipes from the vertical direction, accelerating the evaporation of the water film covered on the outer pipe surface [74]. It was observed from experiments that the tubular structure could provide more uniform water film distribution on the outer surface [75]. Tubular IEC was expected to achieve lower supply air temperature and promote efficient cooling issues. However, the large volume of the device was the reason that constrained its extensive application [76].

Fig. 4 A prototype of the tubular porous cooler [77]

2.4 Counter-cross-flow IEC

The counter-cross-flow IEC usually consists of many thin plates in hexagon shape [78, 79]. Fig. 5(a) reveals a counter-cross cooler with a regular hexagon heat transfer surface [16]. The primary air and secondary air flowed orthogonally at the entrance and the end of channels but switched into a counter-flow pattern in the middle section. Fig. 5(b) is the real object made of aluminum foil. Theoretically, the counter-flow heat transfer area accounts for 58.6%, and the remaining 41.4% area is in cross-flow heat exchange. Experiments were set up to test the cooling effect of this cooler under diverse operating conditions. Produced air temperature increased from 23.9 to 26.2℃ with the inlet air temperature raising from 29.5 to 35.5℃. The dew point effectiveness varied from 58.1% to 71.1%, and the highest COP could reach 13.8. Hence, this proposed cooler was qualified as a pre-cooling device for the residential AC system.

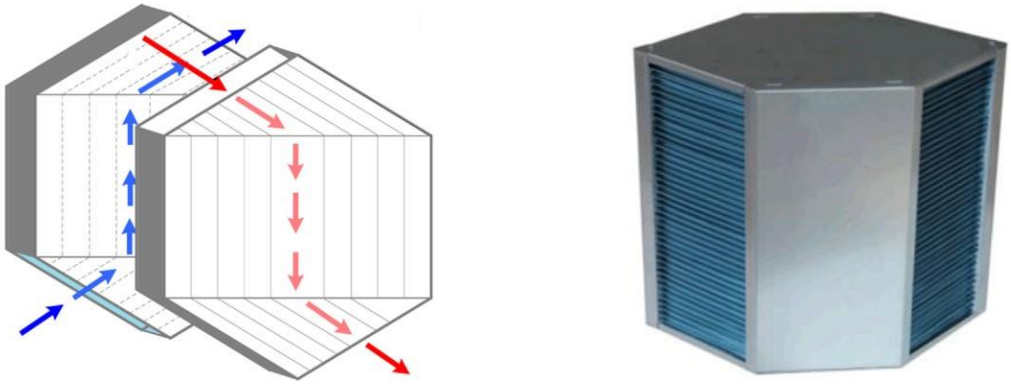

(a) (b)

Fig. 5 (a) 3-D view of the counter-cross-flow IEC (b) Real object of counter-cross-flow IEC [16]

Pandelidis et al. evaluated the application potential of the hexagon DPIEC system by employing the black-box model based on regression equations. The data for the black-box model was originated from the test rig shown in Fig. 6. This study indicated 95% of total cooling load could be covered by DPIEC with 65% of seasonal electricity, which was much efficient than the energy wheel in a hybrid system [80].

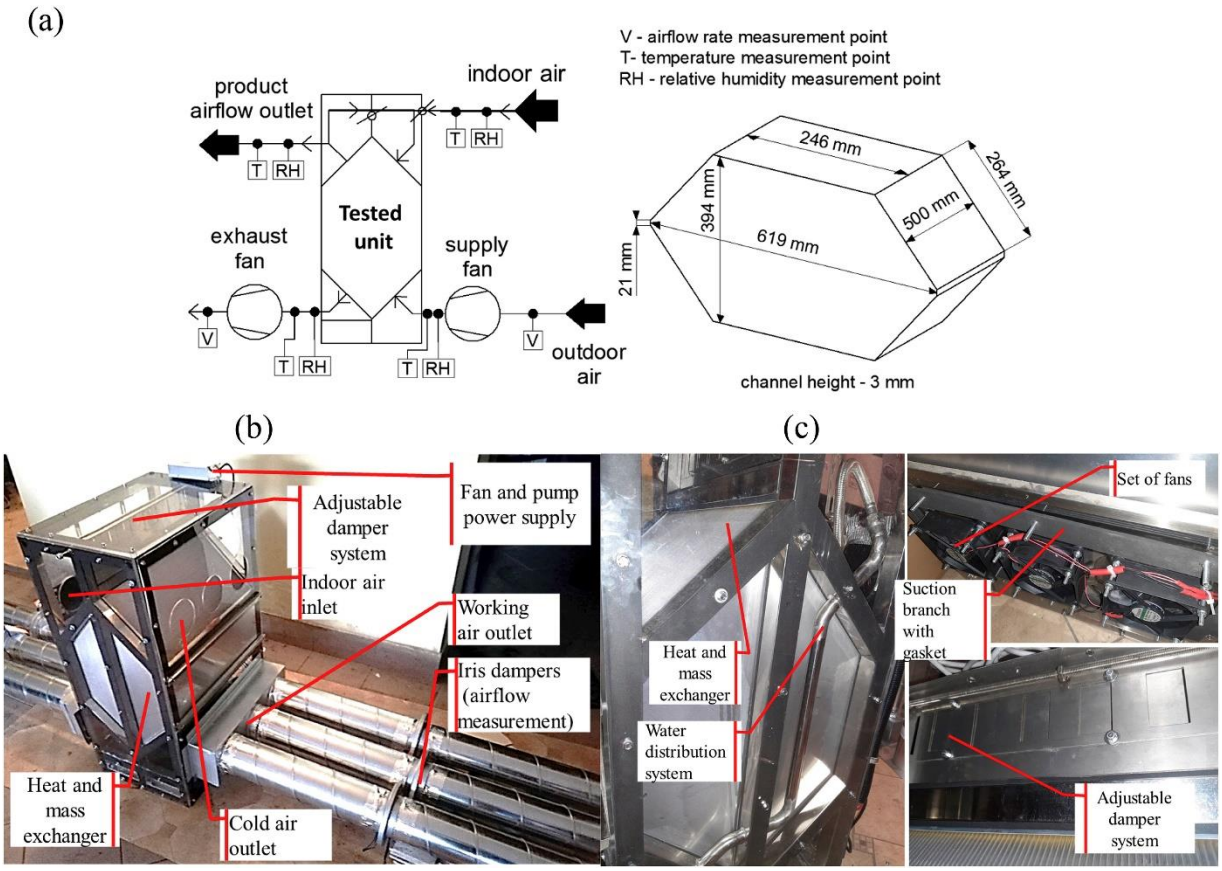

Fig. 6 schematic diagrams of (a) hexagon DPIEC system (b) Real photo of test section (c) Important elements of the unit [80]

2.5 Heat-pipe-based IEC

Heat-pipe-based IEC also attracted attention in the past decades [81-83]. The heat pipe, with considerable thermal conductivity, has been incorporated into IEC for performance enhancement. Fig. 7(a) shows a gravity-assisted heat pipe-based RIEC with the pipes staggered. The section of the heat pipe in the dry channel serves as an evaporator to absorb the heat from the primary air. The other side is equivalent to a condenser, attaching the spraying water on the outer surfaces to generate the water films and removing the heat through evaporation. After the fluid medium in the tube absorbs heat and evaporates into the gas state, gas flows into the condenser due to the saturation pressure difference between the evaporator and condenser. Then, it recovers to the liquid state by heat release in the condenser and then flows back to the evaporator because of the gravity and capillary action for the subsequent circulation. During this process, the heat is taken away by the evaporated water.

Early proposed by Riffat and Zhu (Fig. 7(b)), a mathematical model was built for a heat-pipe-based RIEC that was inserted into a ceramic cylinder water container to cover the condenser in the wet channel [81]. The prototype and the detailed components of a tube module were presented in Fig. 7(c). There are plenty of pores in the container for water permeation. When air sweeps over the container, the siphon action consistently bring water to the container surface for evaporation. This research topic was continued by Amer theoretically and experimentally [84]. The thermal performance, as well as the economic and environmental benefits, was discussed in detail. It was obtained from the experimental data that this heat-pipe-based IEC was able to produce the air within the thermal comfort zone when the

temperature of input ambient air was below 42℃ as well as RH was under 30%. Furthermore, the greater cooling capacity could be obtained by increasing the number of heat pipes if the temperature was above 42℃. It was measured that the COP of the prototype ranged from 4.62 to 13.16, and the wet-bulb effectiveness fluctuated from 0.52 to 1.05.

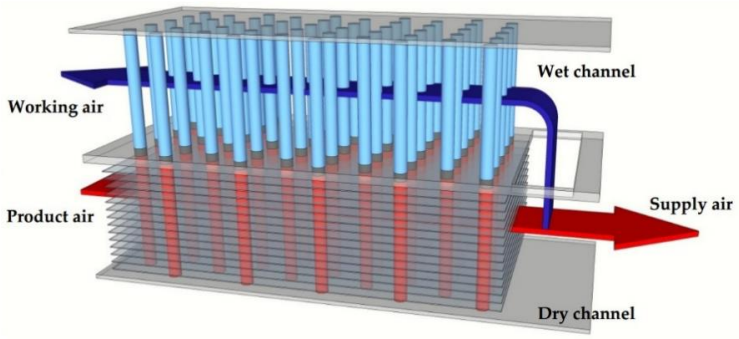

Fig. 7 (a) Schematic diagram of heat-pipe based RIEC [82]

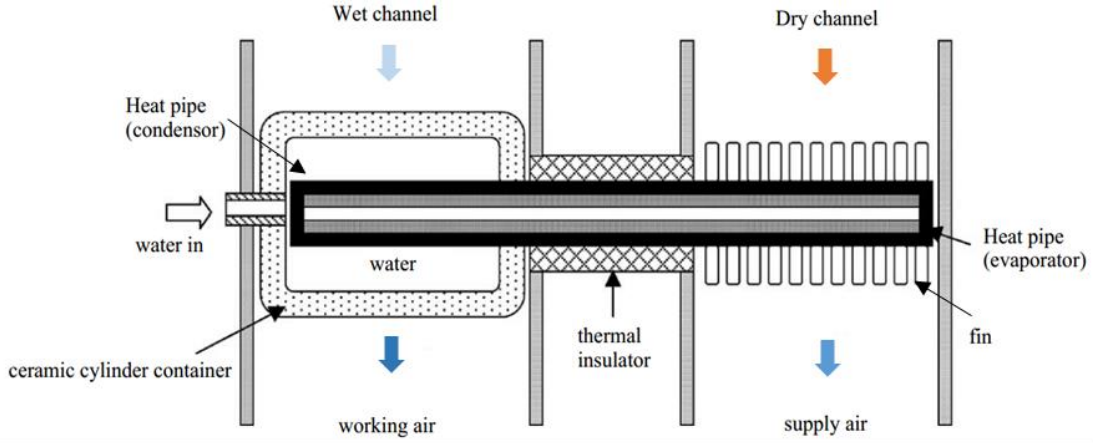

Fig. 7 (b) Schematic diagram of ceramic container and heat-pipe based IEC [81]

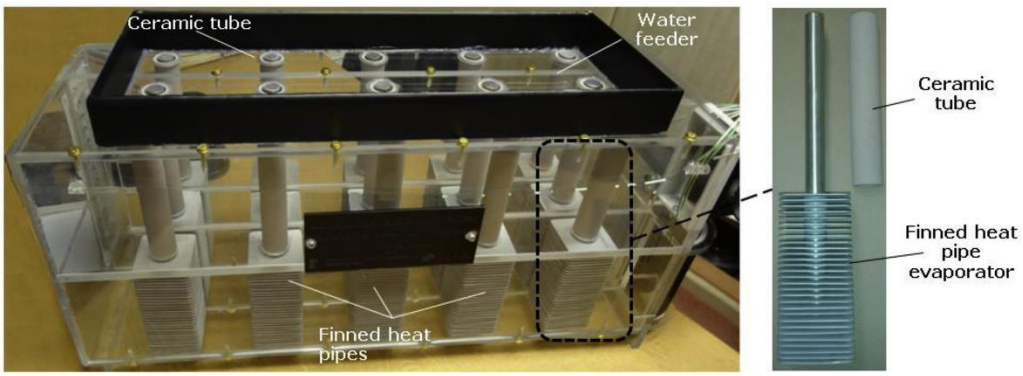

Fig. 7 (c) Prototype of the heat-pipe based RIEC and a tube module [83]

2.6 Internal enhancement structure

2.6.1 Corrugated wick

Some innovative wick structures were proposed to enhance the heat exchange in IEC. The corrugated structure was one of the novel types that was expected to improve cooling efficiency. As depicted in Fig. 8, the corrugated wick could noticeably increase the heat transfer area. They were made from cotton or paper so as to absorb more water for evaporation in the secondary air channel [85]. In a typical IEC, the pressure drop of the air in the dry channel normally was in the range from 60 to 185 Pa,

and it would be 100 to 500 Pa in the wet channel due to the extra resistance from spraying water [75]. As the special structure was introduced, it was aware that the pressure drop of the IEC would increase faster with the volume flow rate. Thus, the trade-off between the improvement of heat transfer and the growth of pressure drop should be taken into consideration in the early design stage. An analytical estimation of pressure drop growth owing to various shapes and dimensions could be found in Ref. [45].

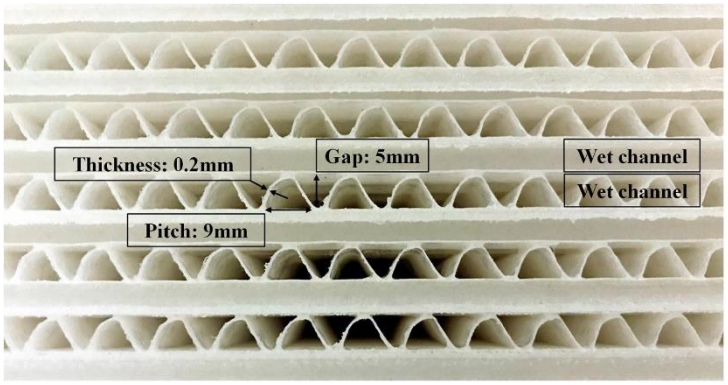

(a) Corrugated wicks in the wet channel [85]

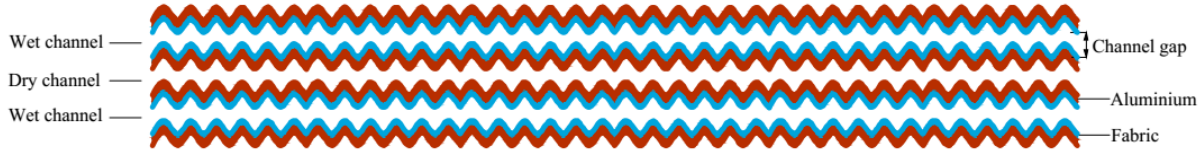

(b) The corrugated shape of channels [86]

Fig. 8 Two corrugated structures in IEC channel

2.6.2 Internal baffle

As shown in Fig. 9, adding baffles is another approach to promote heat exchange because they lead to some small internal vortex in the primary air channel [87]. Referring to the studies by Kabeel et al. [59, 88], the heat transfer coefficient was augmented considerably after incorporating the cooler with baffles. The author investigated the effects of diverse air conditions and optimized the number of baffles arranged in the dry passage. Results demonstrated that the wet-bulb effectiveness for the RIEC with baffles was at least 33.3% higher than the one with smooth surfaces. The temperature drop caused by this IEC increased with the added number of baffles. Detailed convective heat transfer coefficient formulas with baffles in the dry channel will be presented in Table 5.

Besides, according to the local weather conditions, this IEC with internal baffles could be combined with a solar-assisted humidification-dehumidification (HDH) system for both cooling and desalination purposes [89]. Experimental results revealed that the cooling capacity of this hybrid system varied in the range between 253.3 and 417.4W. Meanwhile, it could produce 38.65 L distillate water every day.

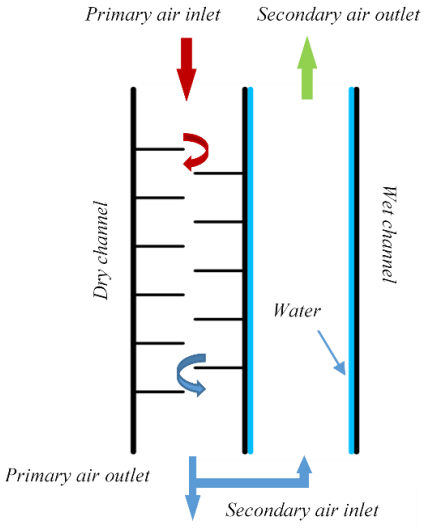

Fig. 9 IEC with baffles (the number of baffles: 11) [59]

2.6.3 Aluminum fin

The aluminum fins were applied in a DPIEC by Ali et al. to increase the heat transfer surface area [90]. Comparative experiments between two prototypes with fins and non-fins, as presented in Fig. 10, were conducted under hot and arid inlet air conditions. Contributed by circular fins in the dry channel surfaces, the cooling capacity was observed a 18% improvement more than the non-fins one.

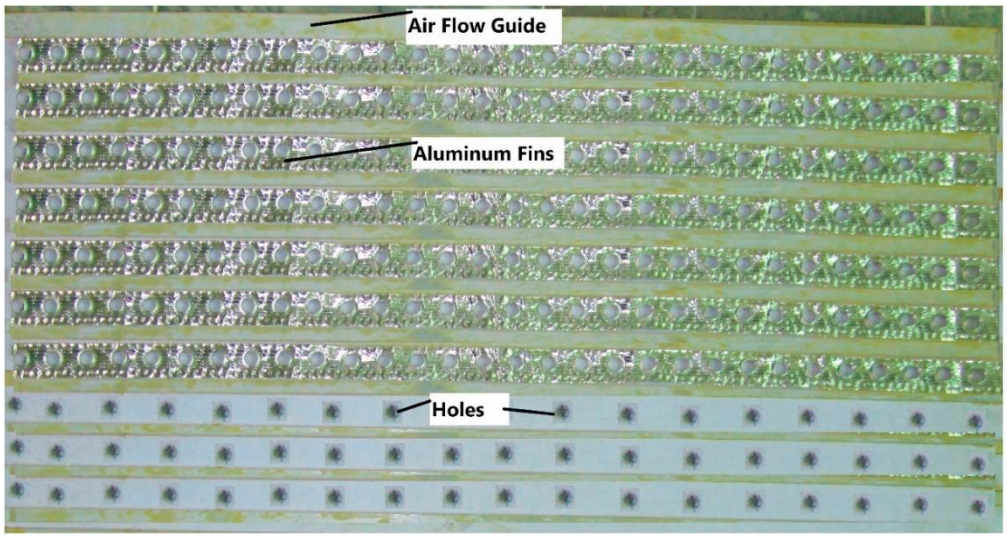

(a)

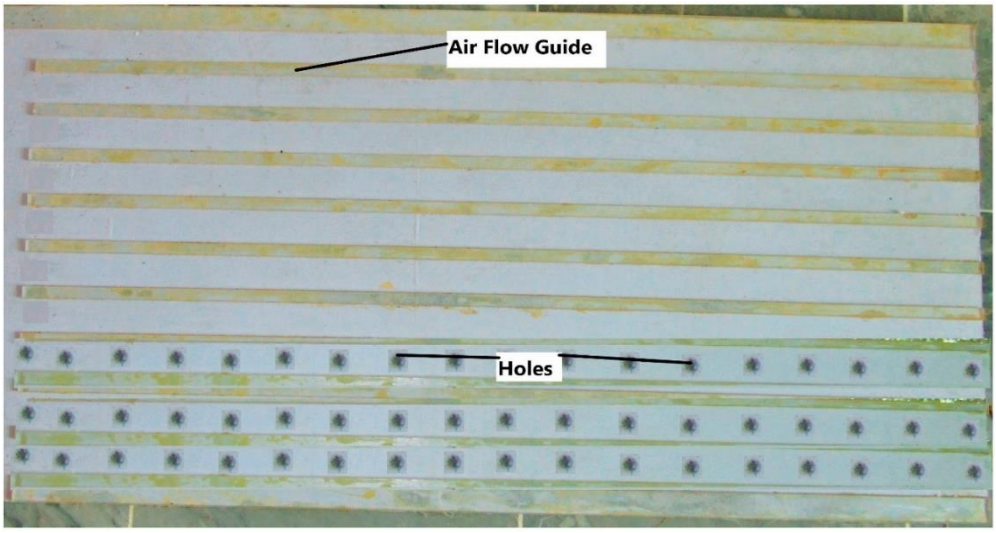

(b)

Fig. 10 Comparison of (a) fins and (b) non-fin dry channel surfaces [90]

2.7 Convective heat transfer coefficient/Nusselt number

The convective heat and mass transfer coefficients need to be determined when establishing the simulation model of IEC. These two parameters are associated with Lewis relationship (Eq. (6)). In other words, if one of them is given, the other one can be worked out. Besides, the convective heat transfer coefficient can be calculated through Eq. (25) and empirical equations. However, the summary of empirical equations is rarely found in the existing published literature. Table 5 presents the popular empirical equations of the Nusselt number or convective heat transfer coefficient applied in IEC research.

$$h = \frac{Nu \cdot \lambda}{d_e} \tag{25}$$

Table 5 Summary of empirical equations of Nusselt number or the convective heat transfer coefficient in previous researches

Author	Method	Type of IECs	Feature	*Nu / h*
Chen [31]	Sim.	Counter-flow	Aluminum foil plate	$h = 0.023\frac{\lambda(\frac{u}{v})^{0.8}Pr^{0.3}}{{d_e}^{0.2}}$
Cui [55]	Sim.	M-cycle counter-flow	-	Heat: $Nu = 2 + 0.6Re^{\frac{1}{2}}Pr^{\frac{1}{3}}$ Mass: $Sh = \frac{h_m D_p}{D_{va}} = 2 + 0.6Re^{\frac{1}{2}}Sc^{\frac{1}{3}}$
Guo [48]	Sim.	Cross-flow	-	$h = 54u^{0.7}$
Kabeel [59, 87]	Sim./Exp.	Counter-flow	With baffles in the primary air passage	$Nu = 0.103 \times Re^{0.759}Pr^{0.4} \times (\frac{L}{s_d})^{0.167} \times \frac{s_h}{s_p}$
Zheng [91]	Sim./Exp.	Cross-flow	aluminum plates	$h = 1.86Re^{\frac{1}{3}}Pr^{\frac{1}{3}}(\frac{d_e}{L})^{\frac{1}{3}}\frac{\lambda}{d_e}$
Liu [92]	Sim.	M-cycle counter-flow	Corrugated surface with fiber in the wet channel	Dry: $Nu = \left[\left(1.49 \cdot \left(\frac{y}{DeRePr}\right)\right)^{4.5} + 8.235^{4.5}\right]^{\frac{1}{4.5}}$ Wet:

				$Nu = 0.1(\frac{l_e}{\delta})^{0.12} Re^{\frac{1}{2}} Pr^{\frac{1}{3}}$
Lin [93]	Sim./Exp.	M-cycle cross-flow	-	Dry: $Nu = 5.60$ Wet: $Nu = 0.1(\frac{l_e}{\delta})^{0.12} Re^{\frac{1}{2}} Pr^{\frac{1}{3}}$
Liberati [94]	Sim.	Cross-flow	-	$h = \frac{\lambda}{d_e} 0.0185 Re^{0.928} Pr^{\frac{1}{3}}$
Li [79]	Sim.	Counter cross flow	aluminum foil	$h = 1.86 Re^{\frac{1}{3}} Pr^{\frac{1}{3}} \left(\frac{d_e}{L}\right)^{\frac{1}{3}} (\frac{\eta_a}{\eta_{w,f}})^{0.14}$
Zhou [95]	Sim.	Cross-flow	Stainless steel plate	$h = 36.31(\rho u)^{0.68} \left(\frac{L}{d_e}\right)^{-0.08}$
Rogdakis [96]	Sim./Exp.	M-cycle	-	$Nu = 3.66 + \frac{0.0668 \cdot d_e/L \cdot Re \cdot Pr}{1 + 0.04 \cdot (d_e/L \cdot Re \cdot \mathrm{Pr})^{\frac{2}{3}}}$
Boukhanouf [97]	Sim./Exp.	Counter-flow regenerative	Porous ceramic	$Nu = 0.664 Re^{\frac{1}{2}} Pr^{\frac{1}{3}}$
Riangvilaikul [8] Chen [98]	Sim.	Counter-flow	Polyurethane; aluminum foil	$Nu = 8.235$
Sun [17]	Sim./Exp.	Tubular	Porous ceramic	Dry: $Nu = \frac{\frac{\lambda_T}{8}(Re - 1000)Pr}{1 + 12.7\sqrt{\frac{\lambda_T}{8}\left(Pr^{\frac{2}{3}} - 1\right)}} \cdot (1 + \frac{2r}{Z})$, $\lambda_T = \frac{1}{[1.82\log(Re) - 1.64]^2}$ Wet: $Nu = a_0(\frac{S_2}{d_0})^{a_1}(\frac{S_3}{d_0})^{a_2}(\frac{S_2}{S_3})^{a_3} R_s{}^{a_4} Re^{a_5} Pr^{\frac{1}{3}}$ $a_0 = 0.55101, a_1 = 9.8464, a_2 = -9.8979$ $a_3 = -9.8556, a_4 = 0.064556$

Note: 1. The convective heat and mass transfer coefficient in this table are used under laminar flow conditions (Re<2300).
2. Sim: Simulation Exp: Experiment

3. Materials

The poor water retention ability and low wettability have been realized as the barrier of reliable evaporation from the wet channel surface. As known from the IEC working principle, the heat is mainly taken away by evaporative latent heat. Suitable materials significantly strengthen the performance because they can keep water film evenly distributed for continuous and stable evaporation [46, 48]. Generally, efforts can be assorted into two aspects. On the one hand, enlarge the heat transfer area to contact with more spraying water. On the other hand, deposit the hydrophilic coating on the wet side surfaces, and the water membrane can be formed homogeneously. Several materials adopted in recent years are reviewed in this section.

3.1 Metal

If the material is unable to disperse water droplets into thin film on the surface, the evaporation rate may fluctuate largely. Thus, the material for IEC was expected to have both good thermal conductivity and surface wettability [99]. Many IEC plates were made of metal such as aluminum, copper, and their alloy. The summary of employed materials in existing studies is presented in Table 6. It can be noticed that aluminum is dominated and broadly applied because of its good thermal conductivity and hydrophilicity. Moreover, the aluminum plate thickness was slight, which could be neglected and considered to have the same temperature as the water film [31, 61].

Table 6 Metal materials selected in IEC studies

Research	Material	Type	Thickness(mm)
[15]	Aluminum	Plate	0.14
[40]	Aluminum	Plate	0.25
[68]	Aluminum	Plate	0.14
[69]	Aluminum	Plate	0.5
[100]	Aluminum	Plate	3
[87]	Aluminum	Plate	0.4
[79]	Aluminum	Plate	0.1
[95]	Stainless steel	Plate	1.5
[101]	Aluminum	Plate	0.15
[102]	Aluminum alloy	Plate	0.15
[103]	Copper	Tube	10

3.2 Porous ceramic

With the progress of manufacturing technique and reduction of manufacturing cost, porous media has been employed to strengthen the heat exchange process since plenty of holes can bring much larger contact area and bothers the boundary layer and flow status [104, 105].

Porous ceramics are being utilized widely due to the high porosity, good thermal conductivity, and corrosion-resistant ability [106]. High porosity brings larger specific surface areas as well as water storage capacity. The good water storage ability makes it possible for the spraying system to operate intermittently so as to decrease the energy consumption of pumps and usage of water resource. Wang et al. conducted an experimental study on a tubular porous ceramic IEC (Fig. 11) [74]. The non-permeable membrane was coated to the surface towards the primary air to avoid water penetration. This ceramic IEC and an aluminum IEC covered with textiles on the outer tube surface were compared. Results demonstrated that porous ceramic IEC could maintain the produced cooling capacity consistently for 100 minutes after 5 minutes thoroughly wetted by spraying water. Therefore, an intermittent spray strategy could be achieved, and the energy cost of the water pump could be saved considerably. Sun et al. supplemented theoretical research of this porous tubular IEC. The length of IEC and spacing distance among tubes were optimized [17].

For porous plate type IEC, the porous ceramic water container was integrated with a sub wet-bulb temperature IEC for space cooling in buildings (Fig.12). A prototype cooler was manufactured for the experiment, which extracted part of the primary air into the wet channel. It was tested that the maximum cooling capacity could come to 225W/m^2, and wet-bulb effectiveness was 102.4%, indicating it as an alternative to the traditional vapor-compression AC system in the hot-arid regions [97].

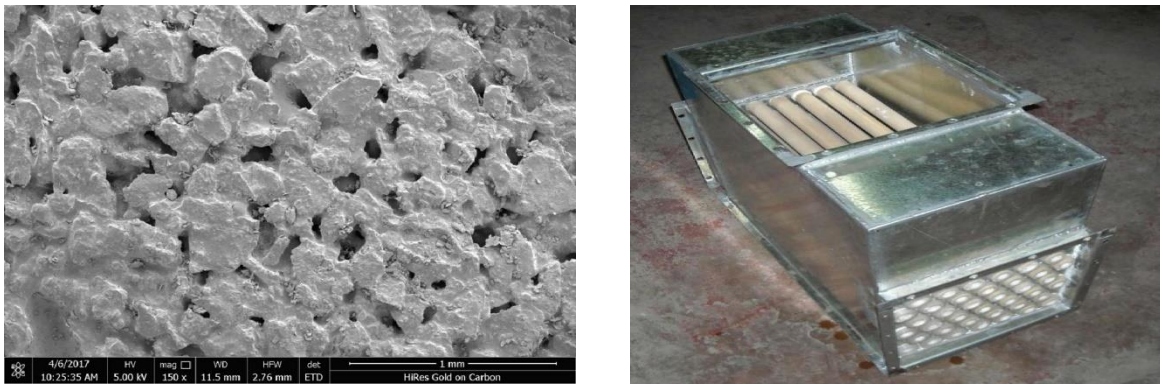

(a) (b)

Fig. 11 (a) Porous ceramic under scanning electron microscope (b) Tubular porous ceramic IEC [17, 74]

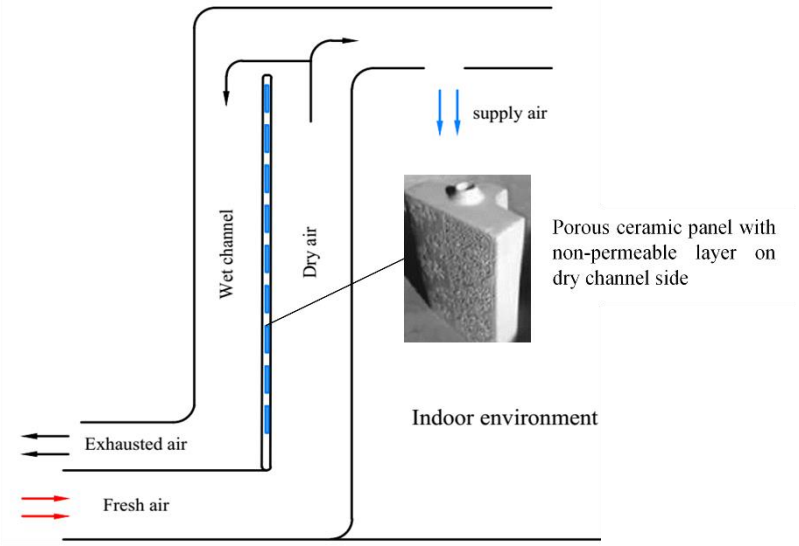

Fig. 12 Schematic diagram of building integrated porous ceramic RIEC [97]

3.3 Materials for surface treatment

The purposes of surface treatment in the dry channel and wet channel are different. Good wettability and water retention ability are required in the wet channel surfaces, while the condensed water is unexpected to stay on the surfaces of the dry channel.

As mentioned in section 2.1.1, evenly distributed thin water film is usually assumed in the wet channel. Nevertheless, large water droplets sometimes cannot disperse to the thin water film due to the surface tension and poor hydrophilicity of the surface material. In order to improve the surface wettability of the wet side, plates towards the secondary air are further treated. Basically, two methods are now technically available and welcomed by researchers. One is to attach materials with strong water-absorbing characteristics. The other is to cover the hydrophilic coating.

The heat and mass transfer on the surface covered with fiber has captured interest in the past few decades [69, 85]. As for the IEC application, some fabrics (textiles) weaved from different fibers were attempted for their moisture-absorbing ability. Test results revealed that the evaporation ability and diffusion ability of the fabrics on the wet channel surface were 77% to 93% and 298% to 396% higher than the smooth surface, respectively [88]. Although most of the fiber materials cannot be directly made as plates for cooler owing to the weak mechanical properties compared with metal and ceramic, they can be fabricated on the base plate surface to increase the heat and mass transfer area and absorb more water. Fiber materials are commonly available in daily life, and the price is affordable. Table 7 shows some combinations of the base plates and attached fiber materials in experimental studies. Duan et al.

not only tested several sets of combinations, but also provided the bonding treatment ways, specifically, hot-melt and adhesive methods [38]. The IEC attached absorbent materials on the secondary channel surfaces was proved to be more effective for evaporation. However, some drawbacks exist and become barriers to the broader application of fiber materials. Firstly, the wetted fiber surface is easy to introduce bacterium and pollute the air and channels, making more troubles for hygiene treatment. Secondly, the life span of them is not long enough so that frequent replacement of the wick is needed, consequently increasing the maintenance cost [99].

Without the risks of breeding bacterium, surface coating technology was employed to promote the formation of the water film. Lee et al. investigated the effect of porous coating on the aluminum surface of a RIEC [107]. Guilizzoni et al. studied two different coatings for IEC, namely, standard epoxy coating (STD) and hydrophilic lacquer (HPHI) [102]. An experimental study was conducted to test the contact angle and water retention ability of them. Photographs revealed that the HPHI led to a lower contact angle than STD, consequently made a significant growth of the hydrophilicity in the wet channel, corresponding to 10% cooling performance improvement.

As mentioned in section 2, condensation occurs in the dry channel when the input outdoor air is hot and humid. Literature has illustrated that filmwise condensation (FWC) was more likely to be generated on hydrophilic surfaces, which led to an additional thermal resistance compared with the hydrophobic surfaces [108, 109]. It has been reported that the condensation on the surface had the tendency to change from dropwise condensation (DWC) to FWC in the evolution process, consequently deteriorating the wet-bulb effectiveness of IEC by 14.8% [110]. Thus, hydrophobic treatment on the primary passage surface was encouraged, increasing the contact angle between water droplet and surface, accordingly improving the droplet drainage ability [2].

To assess the droplet drainage ability of the surface, the condensation area ratio was proposed, which was defined by the ratio of the condensation area and the total heat transfer area (Eq. (26)). According to the visualized studies by Min [2] and Meng [101], the heat transfer effect was bothered by condensed water due to the increased heat resistance. This index was conducive to identify the characteristics of condensation and essential to deeply investigate the impacts of different forms of condensation such as FWC and DWC. Combined with experiment studies, this index would evaluate the droplet removal ability of the plate material.

$$R_{con} = \frac{A_{con}}{A_{tot}} = \frac{A_{FW} + A_{DW}}{A_{tot}} \tag{26}$$

Table 7 Configuration of the base plate and covered material in experiments

Research	Base plate material	Coated material
[16]	Polystyrene	Nylon fiber
[38]	Wax	Kraft paper
[111]	Polyethylene	Fiber sheet
[8, 112]	polyurethane	Cotton sheet
[40]	Aluminum	Porous fiber
[69]	Aluminum	Felt
[86]	Aluminum	fabric
[59]	Aluminum	cotton
[10]	Aluminum	Kraft paper

3.4 Other materials

In addition to metal, porous ceramic, and fiber sheet, some experiments also adopted organic materials such as polystyrene [16], polycarbonate [113], polyurethane [8], polyethylene phthalate [114, 115], PVC [116], cotton sheet [112], clay [117], and polyethylene terephthalate (PET)/cellulose [118] to make the plate type or tubular type coolers. Although their thermal conductivity was lower than metal materials, their thermal resistance was small due to the thin thickness of the plate to satisfy the experimental requirements.

4. Hybrid IEC system

The cooling effectiveness of single-stage IEC is limited by climate conditions, making it not widely used initially. In order to address greater cooling load in buildings, the IEC system has been combined with other AC devices. This section reviews some hybrid systems and novel concepts raised in recent years.

4.1 Multi-stage IEC and IDEC

Multi-stage evaporative system couples one or two IEC and DEC, which is mainly employed in hot and arid regions. Regarding the multi-stage IEC, Moshari et al. simulated two-stage IECs in three airflow configurations based on the weather data of six selected cities of Iran [7]. Dimensionless water evaporation rate was come up to judge the environmental friendliness. This study proved the two-stage IECs could substitute mechanical vapor compression systems and ensure thermal comfort at the same time.

As for the indirect/direct evaporative cooling (IDEC) system, the influential factors have been examined from the perspectives of theoretical modeling, experiments, and field tests. The working principle and psychrometric chart are presented in Fig. 13. In this module, the hot air is sensibly cooled in IEC then chilled by DEC with the increase of moisture content. In the hot-arid area, general mathematical models were developed for this two-stage system, which could be found in Ref. [119] and [120]. Heidarinejad and Moshari studied the two-stage system considering the effect of longitudinal heat conduction and spraying water temperature. Two-stage IDEC, single IEC, and RIEC were compared from aspects of effectiveness and COP [119]. Shirmohammadi and Gilani surveyed the IDEC in nine airflow configurations, indicating that co-current DEC with cross-flow IEC contributed the most outstanding efficiency [120]. Fikri et al. conducted an experimental study of IDEC incorporated with straight heat pipes. When the inlet air temperature was at 45°C and in 0.8m/s velocity, the largest temperature drop was 18.15°C [121]. In the practice of engineering, this system was measured with the average temperature drop by 10°C in a natatorium [122]. Besides, according to a field test result by Huang et al., the energy consumption of the three-stage IDEC system was only 7.4 W/m^2 in a multi-functional building, which was far below 40 W/m^2 of a conventional AC system. The outlet temperature was varied within 14.3°C to 16°C under local weather conditions during the test period. However, this three-stage system occupied much more space for installation, which became the main reason for limited application [123].

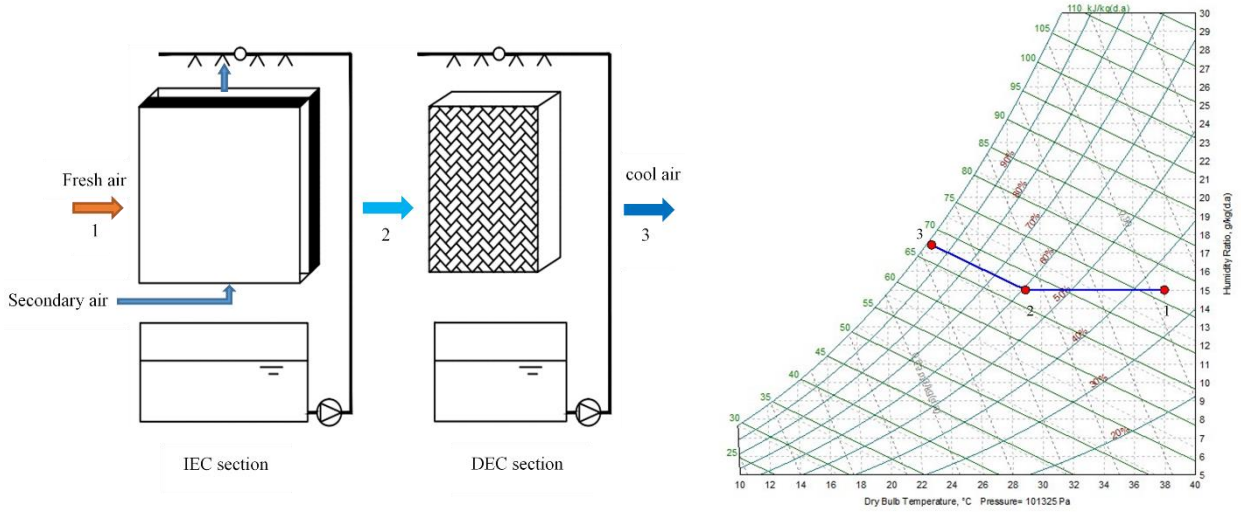

Fig. 13 Schematic diagram and psychrometric chart of two-stage IEC/DEC

4.2 IEC+ heat pump

Li et al. experimentally studied the coupled IEC/heat pump package with multiple modes [124]. As observed in Fig. 14, two sets of water spraying systems can operate individually with the variable climatic conditions. Classified by the off/on status of the water systems, four operation modes can be identified as follows:

Mode 1 (IEC + ECHP): Two water loops is running. Both exhaust air channels of the plate heat exchanger and condenser of the heat pump are wetted by water. In this case, the package serves as an IEC followed by an ECHP. Mode 2 (IEC + HP): Only the water loop of exhaust air channels of the heat exchanger is operating. The package unit consists of an IEC with a regular heat pump module. Mode 3 (SHE + ECHP): Only the condenser of the heat pump is under water spraying. Therefore, the package operates as an air-to-air sensible heat exchanger enhanced by an evaporative condenser heat pump. Mode 4 (SHE + HP): Two water spraying systems are out of service. In such a case, the exhaust air channels and condenser of the heat pump are both in dry states. The prototype could be regarded as the combination of an air-to-air sensible heat exchanger and a regular heat pump.

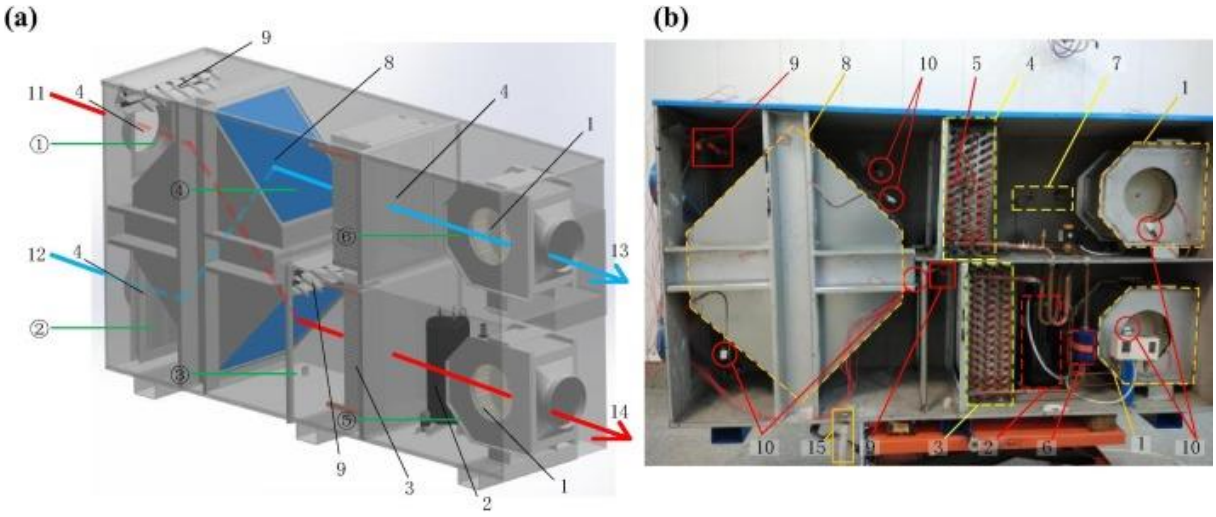

Fig. 14 Structure of hexagon DPIEC with heat pump unit (a) schematic diagram (b) inside view of the actual prototype [124]

4.3 IEC+ mechanical AC device

IEC, with the good cooling effect at the low cost of energy, has been arranged as a pre-cooing device before the mechanical AC device such as air handling unit (AHU) or vapor compression refrigerant system (VCRS) in buildings with large cooling load, which broadened its application scopes from hot-dry areas to temperate or hot-humid regions. Fig. 15 presents the workflow of the combined RIEC/AHU system. When the relative humidity of the fresh inlet air is not high, IEC is responsible for air pre-cooling purpose, and VCRS is used for dehumidication cooling [125]. In order to enhance the cooling effect of IEC, exhausted air from air-conditioned space in the building is introduced as secondary air for energy recovery. The condensation water occurs if the outdoor air was hot and humid, which meant that IEC was not only a pre-cooling device but a pre-dehumidifier.

Delfani et al. developed a model for IEC/PUA system and validated it by experiments. IEC would reduce 70% cooling load against 55% of electricity saved for PUA [126]. Chen et al. simulated the IEC/AHU system under the climate in Hong Kong. The condensate produced by AHU was suggested to be collected and reused as the spraying water for IEC. The annual energy-saving of the IEC pre-cooling section was estimated to be 45% higher than the enthalpy-recovery rotating wheel system [10]. Min et al. carried out on-site measurements of IEC/AHU in a wet market and monitored the monthly cumulative cooling capacity for a whole year. The applicability in eight cities was discussed and predicted [127]. Cui et al. compared the performance of IEC/AHU system in five selected regions with

diverse weather characteristics, indicating that at least 35% of energy could be cut down owing to the installation of the IEC pre-cooling unit [128]. They also supplemented the research to explore the energy-saving potential of the IEC/VCRS system, which revealed that 47% of the cooling load was fulfilled by IEC at the cost of a little additional amount of fan power [129]. ε-NTU model was established to analyze the performance of the IEC/VCRS system under temperate climates considering condensation or non-condensation state [130].

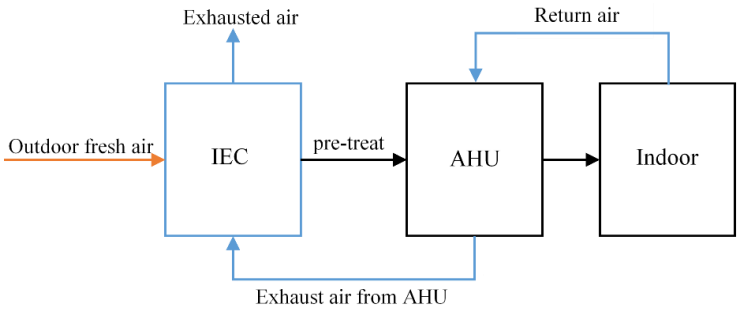

Fig. 15 Schematic diagram of the RIEC followed by AHU [10]

4.4 Radiative cooling + IEC

A hybrid system that coupled a nocturnal radiative cooling (NRC) circuit with IEC was put forward in Tehran, Iran's capital city. In Fig. 16, the water releases heat at night through NRC and is stored in a water tank. In the next daytime period, it is supplied to the cooling coil unit (CCU) for pre-cooling. Comparative studies were numerically conducted for IEC in three modes: outdoor air, pre-cooled air from CCU, and part of primary air from IEC as secondary air (i.e., RIEC), respectively. Results showed that NRC/RIEC performed the best among these three modes, and the effectiveness was more than 45% higher than typical stand-alone RIEC.

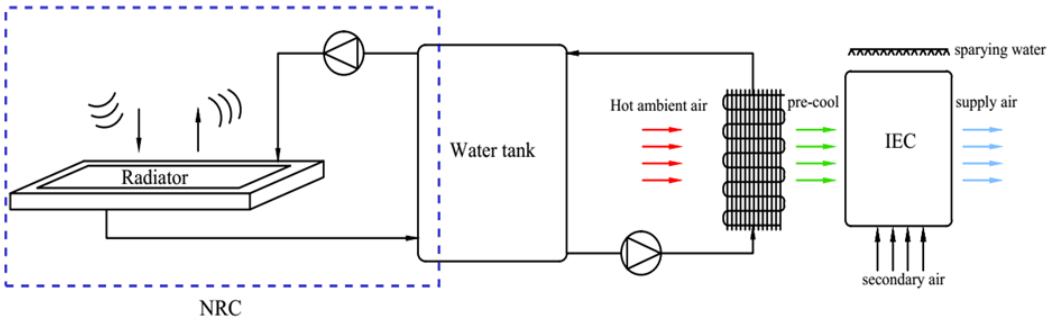

Fig. 16 Schematic diagram of the hybrid NRC/IEC system (use outdoor air as secondary air) [131]

The combination of two passive cooling approaches was also investigated by Katramiz et al. with a closed cycle water reclamation using an air-water harvesting system, and the comparison was conducted between the hybrid system and RC alone (Fig. 17). With the help of the RC section, the water consumption of DPIEC was decreased by 44.2% on average, while the electrical load was 53.4% lower than using typical AC device under cooling period in Kuwait [132].

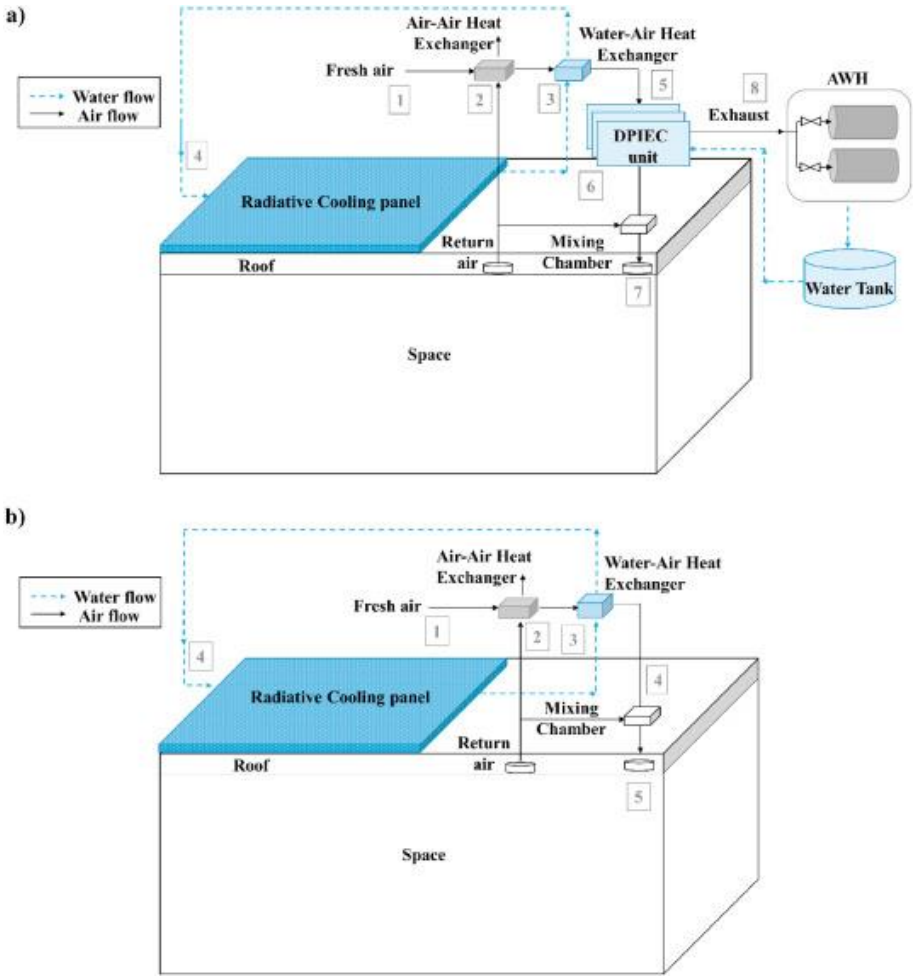

Fig. 17 Schematic diagrams of (a) RC panel + DPIEC (b) RC panel alone [132]

4.5 Ground heat exchanger +IEC

The ground heat exchanger (GHE) usually combines with other ancillary equipment to provide heating and cooling [133-135]. In Fig. 18, the GHE absorbed cooling from underground soil to cool the water. Afterwards, the chilled water was supplied to CCU for the first-stage air cooling. The ambient air passed through the CCU then flowed into IEC for further cooling. It also could be observed that the energy was only consumed by delivering equipment such as water pumps in the whole process. The modules for GHE and IEC were built in Ref. [136]. Due to the auxiliary cooling by GHE, the primary outlet air of IEC could satisfy the cooling requirements and remain steady in arid cities such as Tehran. Furthermore, this hybrid system could achieve about 15% greater effectiveness than NRC/IEC under the same inlet air conditions.

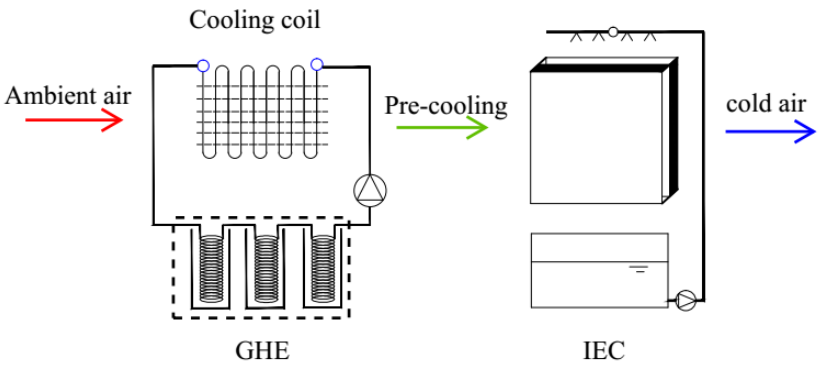

Fig. 18 Schematic diagram of the hybrid GHE/IEC system [136]

Nemati et al. proposed integrating the underground air tunnel with IEC [137]. As depicted in Fig. 19, ambient air is extracted into the secondary channel and the earth-air heat exchanger. For the supply airstream, the surrounding soil absorbs heat from the buried pipes that carried the fresh outdoor air, and IEC is responsible for the further sensible cooling. This coupled system was proved not only to maintain desired indoor thermal comfort but also saved 62% and 45% energy and water consumption, respectively.

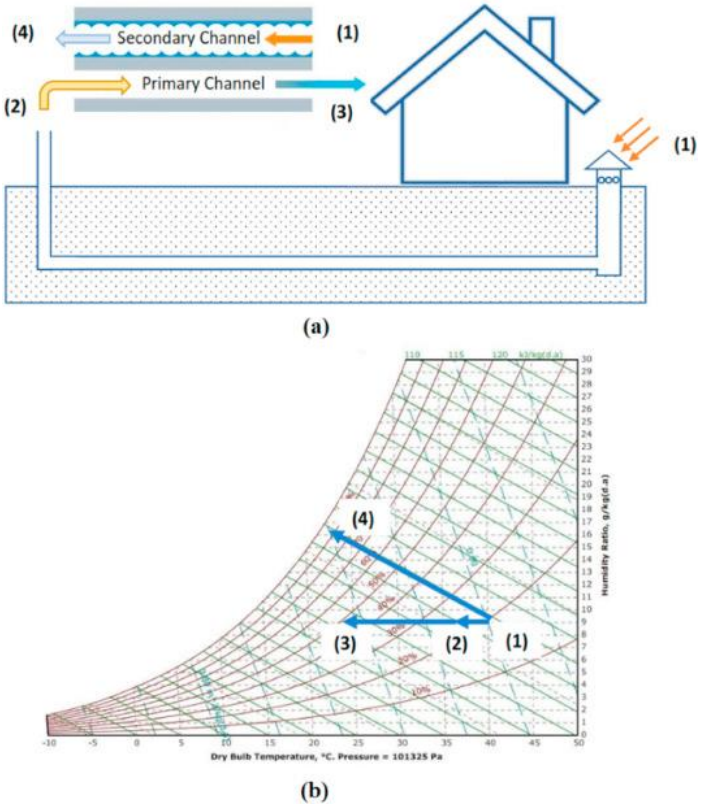

Fig. 19 a) the schematic diagram, b) psychrometric chart for each process [137]

4.6 Dehumidifier + IEC

Liquid desiccant dehumidifier (LDD) [138], solid dehumidifier (SD) [139], and desiccant wheel (DW) [140] are commonly available in AC system. Fig. 20 shows the LDD followed by an IEC to treat the hot and humid fresh air in subtropical regions. The moist outdoor air is dehumidified by the strong solution film of lithium chloride (LiCl) desiccant, which is an isoenthalpy process. Hence the air temperature increases with the decrease of humidity. After passing through the LDD, the hot-dry air is delivered to the RIEC for sensible cooling. In order to obtain a lower outlet temperature, part of primary air or the return air from air-conditioned room is introduced to the wet channel. Cui et al. proposed a cooler that implemented cooling and dehumidification process simultaneously [141] Sohani et al. employed five statistical methods to forecast the performance of LDD/RIEC system. The stepwise regression method was determined as the best approach through the comparison with experimental data [142]. Comparative research between desiccant-enhanced IEC and traditional VAV system was conducted by Lee et al., and the former was estimated to save 10% to 18% energy in summer [143]. A three-stage system that combined LDD/RIEC with DEC was proposed, and the parameter analysis mainly focused on solution self-cycle ratio (Rs), S/P air ratio, regeneration temperature, and inlet air conditions. The system could process the air below 17.9 ℃ with COP of 0.56 [144]. Comino et al. established the model of DW/IEC system and proved it as an alternative to direct expansion (DX) systems. In six tested climate zones, up to 46.8% of energy could be saved by DW/IEC than DX, resulting in a greater COP and lower operation cost [145]. Bang et al. considered microorganism

contamination of AC systems and optimized the design of a LD-IDEC (Fig. 21). The sterilization performance of the in-duct Ultraviolet germicidal irradiation device was measured. Thanks to the reasonable approaches of sterilization, the composite system can be more reliably used in practical engineering projects [146].

Besides, with the increasing awareness of renewable energy usage, the solar system combined with LDD/IEC has been proposed to support good performance and decline the energy consumption of the whole system. Solar heat can be harvested for desiccant regeneration and power generation. For example, Chen et al. numerically investigated a solar-assisted LDD/RIEC system under the subtropical climate, determining the optimal solar collector area and the S/P air ratio. Up to 53.2% of energy could be saved under design conditions [98]. Goldsworthy and White optimized the supply/regeneration air ratio and S/P air ratio to obtain higher system COP for the solar-assisted SD/IEC system [147]. A tri-generation system was established to provide cooling, heating, and electricity simultaneously. Higher effectiveness was acquired by hiring the solar system to fulfill part of energy consumption and mixing the fresh hot air with the cool air exhausted from the indoor built environment [148, 149].

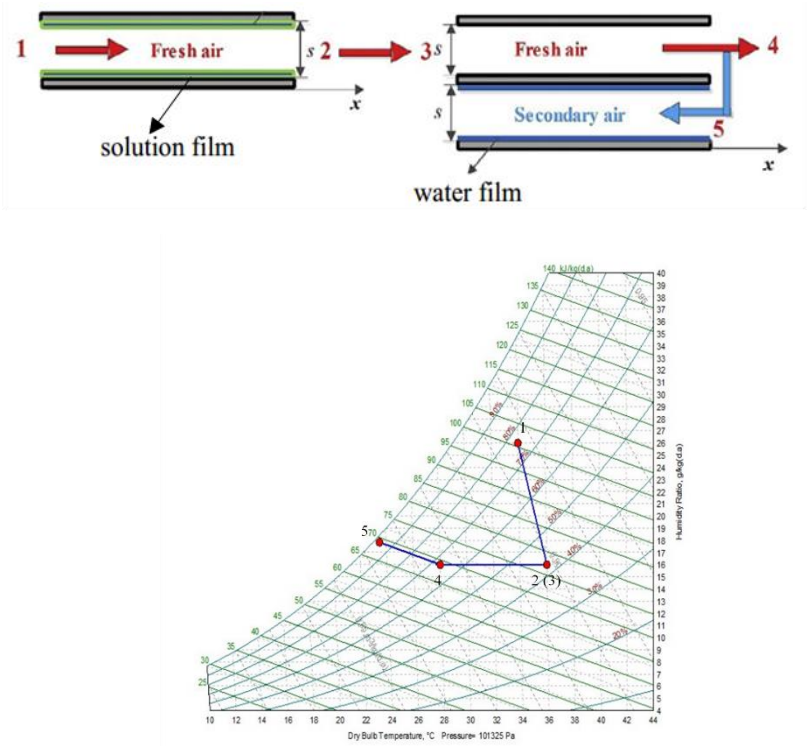

Fig. 20 Schematic diagram and psychrometric chart of LDD/RIEC system [98]

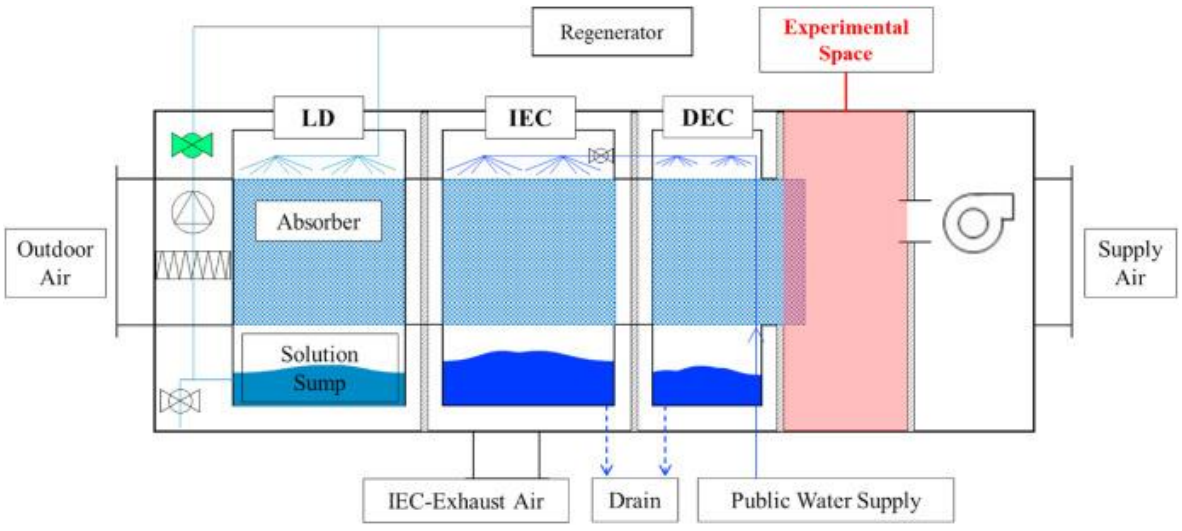

Fig 21. Configuration of LD-IDECOAS [146]

4.7 Ejector cooling + IEC

Driven by the solar heat, the ejector cooling system receives interest with many advantages such as less cooling-related greenhouse gases emission. However, this system is sensitive to the solar radiation intensity, resulting in fluctuations of cooling output. To handle this problem, the solar ejector/IEC system was proposed. The working principle is illustrated as follows.

As shown in Fig. 22, the proposed system consists of three loops: fresh air supply, solar hot water circulation, and refrigerant circulation. Firstly, the fresh outdoor air is introduced to a cross-flow DPIEC. Part of the fresh air is extracted from the dry channel to the wet channel as secondary air. Then the pre-cooled air flows into the evaporator for further cooling, and the thoroughly chilled air is supplied to the indoor space for satisfying the thermal comfort of occupants. In the refrigerant circulation, the refrigerant is processed in the generator to the status with high temperature and pressure through the hot water heated by the solar system. Afterward, the fluid from the generator flows into the ejector, mixing with the low-temperature and low-pressure refrigerant from the evaporator. The mixture is ejected to the condenser accordingly. The first air-cooled condenser absorbs the heat with the help of the cool air from indoor space and secondary air of IEC, following by a second-stage water-cooled condenser to ensure sufficient condensation. Finally, the condensed fluid is divided into two streams. One is pumped to the generator for the next circulation, and the other is supplied to the evaporator for fulfilling the cooling purpose after passing the expansion valve.

Referring to the existing literature, this solar ejector/IEC system was able to output 18℃ cool air, meanwhile, achieved 44% of reduction in the electricity consumption compared with conventional mechanical vapor compression AC system [150]. The maximum COP would reach 13.69 in semi-arid regions [151].

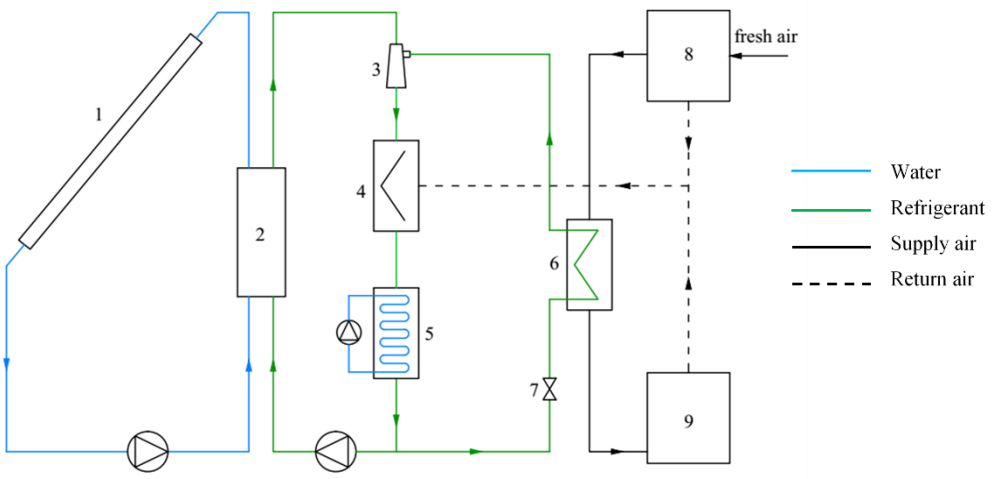

1 Solar collector
2 Generator
3 Ejector
4 Condenser (air-cooled)
5 Condenser (water-cooled)
6 Evaporator
7 Expansion valve
8 IEC
9 Indoor space

Fig. 22 Schematic diagram of hybrid solar ejector cooling/IEC system [150]

5. Other research

As mentioned in the previous sections, IEC has been investigated from perspectives such as the configurations, materials, and multi-stage hybrid system. In order to optimize the application of IEC in practice, researchers have also made efforts in the water spraying system design and IEC system control.

5.1 Studies of water spraying system

The wettability of secondary air surface is one of the most influential IEC thermal performance factors, which is affected by the water distribution system [77, 152]. As mentioned in section 2.1.1, the water film is assumed to cover the surface evenly and completely in the numerical studies. Nevertheless, this is not easy to be achieved in experiments or engineering. Therefore, the spraying system should be designed carefully to minimize experimental errors by proper distribution arrangement. Generally, the secondary air and water-spray direction should be in counter pattern [153]. Recently, in respect to theoretical studies, Lacour et al. established a 3-D model by CFD to calculate the temperature and humidity distribution during the process of spray water dispersion. The spray radius, nozzle aperture, water, and air velocities, and the optimal distance between the nozzle and heat exchanger were discussed [154]. Montazeri et al. simulated spray water behavior in an evaporative cooling system and successfully validated it by wind tunnel test within 10% discrepancy [155].

Apart from theoretical analysis, experiments aiming to optimize the system design were also carried out. Ahmed et al. conducted several experiments under varied air velocities and temperature, focusing on three spraying modes: external mode, internal mode, and mixed mode. The internal spraying strategy was ultimately identified as an effective approach to enhance the heat and mass exchange for the hexagonal plate cooler [116]. De Antonellis et al. analyzed the impact of water nozzles position and airflow directions on performance for a cross-flow IEC. Six configurations were shortlisted for evaluation. As depicted in Fig. 23, top and horizontal spraying configurations were recommended for ideal water distribution [152]. Sun et al. tested five types of spraying nozzles, namely, spiral, conical, square, sector, and target impact nozzles. Nozzles were arranged on the top side (Fig. 24(c)). Both target impact nozzle (Fig. 24(a)) and the spiral nozzle (Fig. 24(b)) had good coverage ratio and uniformity. However, it was found that the target impact type consumed a large amount of water, which may not be suitable in the regions lacking water resources. Therefore, the spiral type was suggested as the optimal choice [77].

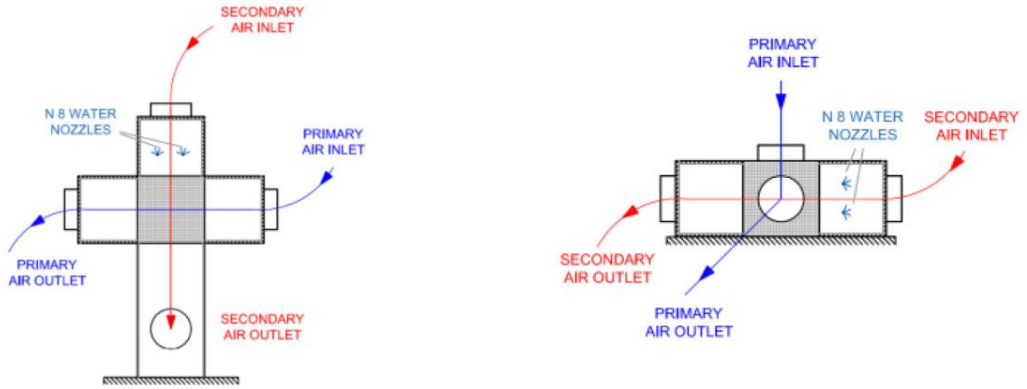

(a) (b)

Fig. 23 System configuration in (a) Top arrangement (b) Horizontal arrangement [152]

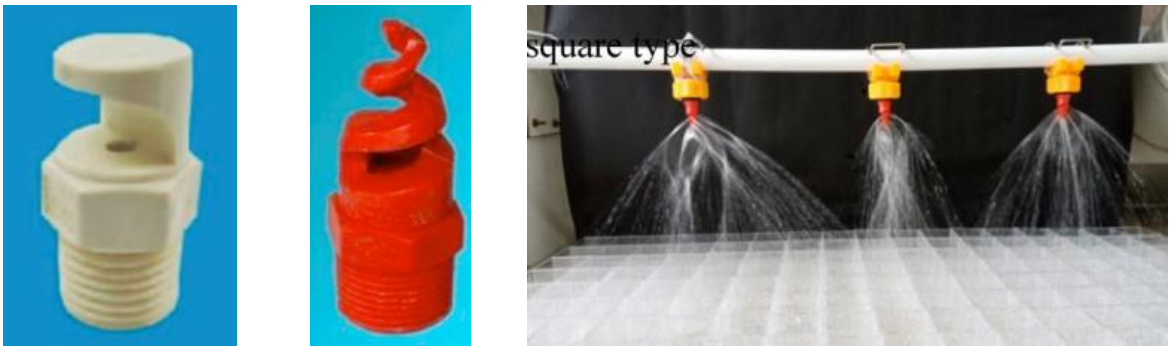

(a) (b) (c)

Fig. 24 (a) Target impact nozzle (b) Spiral nozzle (c) Spraying effect of the spiral nozzle [77]

5.2 Studies of system control

Various control methods [156-158] were proposed for the traditional AC system in different kinds of building to achieve good robustness [159] and accurate control [160-162]. However, the optimal control studies related to IEC were hardly found, although the thermal performance is affected by many factors.

Similar to the conventional AC system, the IEC system can be divided into a water system and an air system, equipped with water pumps and fans, respectively. For both primary and secondary air systems, on-off control is commonly adopted. However, the variable ambient air conditions can lead to a large fluctuation and influence the thermal comfort of indoor environment. To deal with this problem, high-low control was proposed based on variable speed technology to substitute on-off control. Chen et al. coupled the high-low control method with Predicted Mean Vote to examine the energy-saving performance and thermal comfort of the IEC air system [163]. The annual simulation of high-low control strategy revealed that better thermal comfort was achieved against 11.3% energy saving [164]. In order to optimize the high-low control scheme, a proportional-integral (PI) law based on variable speed fans is employed to maintain a stable primary air outlet temperature [63]. The energy consuption of this method was 50% less than standard on-off control, providing a solution for IEC to be applied in occasions that required accurate and stable temperature. Sohani put forward an hourly optimization strategy (HOS) that can make the fans and water pumps operate properly considering inlet parameters, objective functions, and other constraints such as thermal comfort [165]. Compared with the typical operation strategy, 36.2% of operation cost could be cut down with 17.8% enhancement of COP through HOS.

Concerning the IEC water system, the spraying system usually operates continuously to ensure the wetted surfaces in secondary passages. Based on the porous media IEC, intermittent spraying strategies start to be studied. With good water retention ability, there is no need to spray water all the time so that the water resource and the power of water pumps can be saved. The exact spraying and intermittent period depend on the porous material's property, which could be determined through experiments. Concluded by Wang et al., the energy consumption of the water pump in the porous IEC system was only 5% in comparison with the simple IEC system [74, 77].

6. Current research gaps and challenges

From the perspective of modeling, according to the existing literature, studies on the development of 1-D and 2-D models can be found for theoretical analysis of both counter flow and cross flow IEC in recent years. Nonetheless, there still some work that remains to be supplemented on the numerical model of IEC. It has been realized that 2-D model can show the temperature or moisture content distribution in the airflow direction. Therefore the temperature and humidity uniformity of air profile along the channel width direction were required to be simplified as constant. In fact, these air properties are different at each point, so it is necessary to develop more 3-D models in this field.

In respect to the mass transfer behavior, evaporation and condensation need to be mentioned. In the wet channel, water film for evaporation is usually assumed to be steady and uniform, while it is difficult to achieve in practice due to the shrinkage characteristic of the falling liquid and the air velocity [166, 167]. To deal with these problems, the surface wettability factor has been proposed based on selected constant values to discuss the effect. Nevertheless, revised models considering the nonuniformity of the dynamic water film during the evaporation process are still complicated and challenging.

In the dry channel, outlet air properties are influenced by DWC and FWC simultaneously when IEC serves in hot and humid districts, and these two condensation states are also dynamic with falling or retention behavior, which is demanding to predict. In addition, the heat and mass transfer process is influenced by the condensation mechanism varied with different surface characteristics. Thus it needs to be concerned by category. In field applications, studies related to the collection, treatment and utilization of the accumulated condensate are yet to be undertaken.

Referring to the different features in adjacent channels, the surface on one side is required to be hydrophilic for increasing the wetted area for evaporation, while the other side is expected to be hydrophobic for better condensation drainage ability. So far, the heat transfer plate with different functional surfaces is rarely available.

Last but not least, researchers have proposed diversified concepts and simulations of IEC hybrid systems, whereas some integrated experiments or field tests remain to be enriched to promote the system optimizations and applications in the real engineering project.

7. Conclusion

IEC has been developed rapidly with the advantages of low energy consumption and low greenhouse gases emission. Normal counter- and cross-flow IECs have been numerically and experimentally investigated in the past few decades. This study provides an overview of IEC configurations, modeling, materials, novel hybrid IEC systems, and some optimization studies about the design of the spraying system and control strategy. Theoretical studies of IEC are sufficient and detailed from many aspects such as input air parameters, geometric shape and size, airflow arrangement, novel internal structures, as well as system combinations.

Poor surface wettability in the wet channel, to some extent, has been solved by attaching absorbent materials and covering hydrophilic coating. Internal novel structures such as fins and corrugated wicks were embedded into IEC to expand heat transfer and water contact area. Porous materials have shown promising potential to improve wettability. The optimal design of the IEC water spraying system could also lead to better wettability, which consists of counter-flow vertical direction in wet channel and nozzles with good coverage ratio and uniformity,

Single-stage IEC and multi-stage IEC/DEC could substitute mechanical AC systems in some hot-dry regions. However, an IEC needs to be combined with other AC devices such as AHU, LD, and GHE for satisfying the cooling requirement of buildings with a large load in hot-humid areas. In such a situation, when the exhausted air from indoor air-conditioned space is used as secondary air, the IEC is regarded as air pre-cooling equipment at the cost of less electrical energy, accompanied by the condensation in the primary air channel.

Finally, the fan and pump control strategies have been upgraded. On/off control of fans was replaced by high/low or personalized PI control. The constant speed water pump was suggested to operate in a specific interval in the porous tubular IEC system. Hence water and electricity, to a great extent, were saved.

8. Future works and potential opportunities

Referring to the current situations of IEC studies, future works could turn to the following viewpoint: Firstly, the 3-D model that reflects the profile of air properties in IEC is aimed to be developed. Research about the feasibility and field applications of hybrid systems is to be enriched. Secondly, it is necessary to explore long-life materials with good water retention ability and low cost, which are conducive to IEC commercialization. For example, a novel multilayer heat transfer plate may be manufactured with hydrophilic and hydrophobic surfaces to enhance the evaporation and condensation drainage, respectively.

Porous materials are anticipated to be applied for plate-type IEC. For the IEC systems based on porous materials, the trade-off between the heat transfer improvement and the pressure drop added needs to be comprehensively considered.

Last but not least, depending on the water storage capacity of the porous material, intermittent spraying is likely to be realized during the operation period in a plate-type IEC system. Furthermore, the control strategy for water pumps and fans can be more economical. In brief, the consumption of water resources and circulation energy demand could be further reduced.

Acknowledgments

The authors wish to acknowledge the financial support provided by the General Research Fund projects of the Hong Kong Research Ground Council (Ref. No.: 15213219 and 15200420).

References

[1] Wu T, Cao B, Zhu Y. A field study on thermal comfort and air-conditioning energy use in an office building in Guangzhou. Energy and buildings. 2018;168:428-37.
[2] Min Y, Chen Y, Yang H, Guo C. Characteristics of primary air condensation in indirect evaporative cooler: Theoretical analysis and visualized validation. Building and Environment. 2020;174.
[3] Spandagos C, Ng TL. Equivalent full-load hours for assessing climate change impact on building cooling and heating energy consumption in large Asian cities. Applied Energy. 2017;189:352-68.
[4] IEA. The Future of Cooling in China. IEA. https://www.iea.org/reports/the-future-of-cooling-in-china; 2019 [accessed 31 May, 2020].
[5] She X, Cong L, Nie B, Leng G, Peng H, Chen Y, et al. Energy-efficient and -economic technologies for air conditioning with vapor compression refrigeration: A comprehensive review. Applied Energy. 2018;232:157-86.
[6] IEA. The Future of Cooling. IEA. https://www.iea.org/reports/the-future-of-cooling; 2018 [accessed 10 June 2020].
[7] Moshari S, Heidarinejad G, Fathipour A. Numerical investigation of wet-bulb effectiveness and water consumption in one-and two-stage indirect evaporative coolers. Energy Conversion and Management. 2016;108:309-21.
[8] Riangvilaikul B, Kumar S. Numerical study of a novel dew point evaporative cooling system. Energy and Buildings. 2010;42(11):2241-50.
[9] Al Horr Y, Tashtoush B, Chilengwe N, Musthafa M. Operational mode optimization of indirect evaporative cooling in hot climates. Case Studies in Thermal Engineering. 2020;18.
[10] Chen Y, Luo Y, Yang H. Fresh Air Pre-cooling and Energy Recovery by Using Indirect Evaporative Cooling in Hot and Humid Region – A Case Study in Hong Kong. Energy Procedia. 2014;61:126-30.
[11] Jia C, Huang X, Tian Z, Liu Z, Jin Y. Application research of indirect evaporative cooling technology in data centers at home and abroad. Refrigeration and Air Conditioning. 2020;20(1):61-7.
[12] Jain JK, Hindoliya DA. Energy saving potential of indirect evaporative cooler under Indian climates. International Journal of Low-Carbon Technologies. 2016;11(2):193-8.
[13] González Cruz E, Krüger E. Evaluating the potential of an indirect evaporative passive cooling system for Brazilian dwellings. Building and Environment. 2015;87:265-73.
[14] Lin J, Wang RZ, Kumja M, Bui TD, Chua KJ. Multivariate scaling and dimensional analysis of the counter-flow dew point evaporative cooler. Energy Conversion and Management. 2017;150:172-87.
[15] De Antonellis S, Joppolo CM, Liberati P, Milani S, Molinaroli L. Experimental analysis of a cross flow indirect evaporative cooling system. Energy and Buildings. 2016;121:130-8.
[16] Jia L, Liu J, Wang C, Cao X, Zhang Z. Study of the thermal performance of a novel dew point evaporative cooler. Applied Thermal Engineering. 2019;160.
[17] Sun T, Huang X, Qu Y, Wang F, Chen Y. Theoretical and experimental study on heat and mass transfer of a porous ceramic tube type indirect evaporative cooler. Applied Thermal Engineering. 2020;173.
[18] Cui X, Mohan B, Islam MR, Chua KJ. Investigating the energy performance of an air treatment incorporated cooling system for hot and humid climate. Energy and Buildings. 2017;151:217-27.
[19] Pedrazzi S, Allesina G, Muscio A. Indirect evaporative cooling by sub-roof forced ventilation to counter extreme heat events. Energy and Buildings. 2020;229.
[20] Pandelidis D, Anisimov S, Rajski K, Brychcy E, Sidorczyk M. Performance comparison of the advanced indirect evaporative air coolers. Energy. 2017;135:138-52.
[21] Pandelidis D, Cichoń A, Pacak A, Drąg P, Drąg M, Worek W, et al. Water desalination through the dewpoint evaporative system. Energy Conversion and Management. 2021;229.
[22] Raza HMU, Sultan M, Bahrami M, Khan AA. Experimental investigation of evaporative cooling systems for agricultural storage and livestock air-conditioning in Pakistan. Building Simulation. 2020;14(3):617-31.
[23] Xuan YM, Xiao F, Niu XF, Huang X, Wang SW. Research and application of evaporative cooling in China: A review (I) – Research. Renewable and Sustainable Energy Reviews. 2012;16(5):3535-46.
[24] Xuan YM, Xiao F, Niu XF, Huang X, Wang SW. Research and applications of evaporative cooling in China: A review (II)—Systems and equipment. Renewable and Sustainable Energy Reviews. 2012;16(5):3523-34.
[25] Panchabikesan K, Vellaisamy K, Ramalingam V. Passive cooling potential in buildings under various climatic conditions in India. Renewable and Sustainable Energy Reviews. 2017;78:1236-52.
[26] Mahmood MH, Sultan M, Miyazaki T, Koyama S, Maisotsenko VS. Overview of the Maisotsenko cycle – A way towards dew point evaporative cooling. Renewable and Sustainable Energy Reviews. 2016;66:537-55.
[27] Mohammad AT, Mat SB, Sulaiman MY, Sopian K, Al-abidi AA. Historical review of liquid desiccant evaporation cooling technology. Energy and Buildings. 2013;67:22-33.
[28] Yang Y, Cui G, Lan CQ. Developments in evaporative cooling and enhanced evaporative cooling - A review. Renewable and Sustainable Energy Reviews. 2019;113.

[29] Cuce PM, Riffat S. A state of the art review of evaporative cooling systems for building applications. Renewable and Sustainable Energy Reviews. 2016;54:1240-9.
[30] Min Y, Chen Y, Yang H. Numerical study on indirect evaporative coolers considering condensation: A thorough comparison between cross flow and counter flow. International Journal of Heat and Mass Transfer. 2019;131:472-86.
[31] Chen Y, Yang H, Luo Y. Indirect evaporative cooler considering condensation from primary air: Model development and parameter analysis. Building and Environment. 2016;95:330-45.
[32] Baakeem SS, Orfi J, Mohamad A, Bawazeer S. The possibility of using a novel dew point air cooling system (M-Cycle) for A/C application in Arab Gulf Countries. Building and Environment. 2019;148:185-97.
[33] Khalid O, Butt Z, Tanveer W, Rao HI. Design and experimental analysis of counter-flow heat and mass exchanger incorporating (M-cycle) for evaporative cooling. Heat and Mass Transfer. 2016;53(4):1391-403.
[34] Oh SJ, Shahzad MW, Burhan M, Chun W, Kian Jon C, KumJa M, et al. Approaches to energy efficiency in air conditioning: A comparative study on purge configurations for indirect evaporative cooling. Energy. 2019;168:505-15.
[35] Pandelidis D, Anisimov S, Worek WM. Comparison study of the counter-flow regenerative evaporative heat exchangers with numerical methods. Applied Thermal Engineering. 2015;84:211-24.
[36] Lin J, Bui DT, Wang R, Chua KJ. On the fundamental heat and mass transfer analysis of the counter-flow dew point evaporative cooler. Applied Energy. 2018;217:126-42.
[37] Cui X, Islam MR, Chua KJ. An experimental and analytical study of a hybrid air-conditioning system in buildings residing in tropics. Energy and Buildings. 2019;201:216-26.
[38] Duan Z, Zhao X, Zhan C, Dong X, Chen H. Energy saving potential of a counter-flow regenerative evaporative cooler for various climates of China: Experiment-based evaluation. Energy and Buildings. 2017;148:199-210.
[39] Nie J, Yuan S, Fang L, Zhang Q, Li D. Experimental study on an innovative enthalpy recovery technology based on indirect flash evaporative cooling. Applied Thermal Engineering. 2018;129:22-30.
[40] Duan Z, Zhan C, Zhao X, Dong X. Experimental study of a counter-flow regenerative evaporative cooler. Building and Environment. 2016;104:47-58.
[41] Wan Y, Huang Z, Soh A, Cui X, Chua KJ. Analysing the transport phenomena of novel dew-point evaporative coolers with different flow configurations considering condensation. International Journal of Heat and Mass Transfer. 2021;170.
[42] Wan Y, Lin J, Chua KJ, Ren C. Similarity analysis and comparative study on the performance of counter-flow dew point evaporative coolers with experimental validation. Energy Conversion and Management. 2018;169:97-110.
[43] Wang L, Zhan C, Zhang J, Zhao X. Optimization of the counter-flow heat and mass exchanger for M-Cycle indirect evaporative cooling assisted with entropy analysis. Energy. 2019;171:1206-16.
[44] Halasz B. A general mathematical model of evaporative cooling devices. Revue Générale de Thermique 1998;37 (4):245–55.
[45] Moshari S, Heidarinejad G. Analytical estimation of pressure drop in indirect evaporative coolers for power reduction. Energy and Buildings. 2017;150:149-62.
[46] Ren C, Yang H. An analytical model for the heat and mass transfer processes in indirect evaporative cooling with parallel/counter flow configurations. International Journal of Heat and Mass Transfer. 2006;49(3-4):617-27.
[47] Chen Y, Luo Y, Yang H. A simplified analytical model for indirect evaporative cooling considering condensation from fresh air: Development and application. Energy and Buildings. 2015;108:387-400.
[48] Guo CX, Zhao TS. A parametric study of an IEC air cooler. International Communications in Heat and Mass Transfer. 1998;25(2):217-26.
[49] Jradi M, Riffat S. Experimental and numerical investigation of a dew-point cooling system for thermal comfort in buildings. Applied Energy. 2014;132:524-35.
[50] Jafarian H, Sayyaadi H, Torabi F. A numerical model for a dew-point counter-flow indirect evaporative cooler using a modified boundary condition and considering effects of entrance regions. International Journal of Refrigeration. 2017;84:36-51.
[51] Nusselt W. Die oberflachenkondensation des wasserdampfes, VDI Z. 60. 1916;28:569-75.
[52] Cui X, Chua KJ, Yang WM, Ng KC, Thu K, Nguyen VT. Studying the performance of an improved dew-point evaporative design for cooling application. Applied Thermal Engineering. 2014;63(2):624-33.
[53] Wan Y, Ren C, Xing L. An approach to the analysis of heat and mass transfer characteristics in indirect evaporative cooling with counter flow configurations. International Journal of Heat and Mass Transfer. 2017;108:1750-63.
[54] Xu P, Ma X, Diallo TMO, Zhao X, Fancey K, Li D, et al. Numerical investigation of the energy performance of a guideless irregular heat and mass exchanger with corrugated heat transfer surface for dew point cooling. Energy. 2016;109:803-17.

[55] Cui X, Chua KJ, Yang WM. Numerical simulation of a novel energy-efficient dew-point evaporative air cooler. Applied Energy. 2014;136:979-88.
[56] Wan Y, Soh A, Shao Y, Cui X, Tang Y, Chua KJ. Numerical study and correlations for heat and mass transfer coefficients in indirect evaporative coolers with condensation based on orthogonal test and CFD approach. International Journal of Heat and Mass Transfer. 2020;153.
[57] You Y, Jiang H, Lv J. Analysis of influence of IEC heat exchanger based on CFD method. Energy Procedia. 2019;158:5759-64.
[58] Xia Y-F, Zhang H, Lu J, Bao W-B. 3D numerical simulation of indirect evaporative cooler by CFD method. Shenyang Gongye Daxue Xuebao (Journal of Shenyang University of Technology). 2006;28(4):466-70.
[59] Kabeel AE, Abdelgaied M. Numerical and experimental investigation of a novel configuration of indirect evaporative cooler with internal baffles. Energy Conversion and Management. 2016;126:526-36.
[60] Min Y, Chen Y, Yang H. A statistical modeling approach on the performance prediction of indirect evaporative cooling energy recovery systems. Applied Energy. 2019;255.
[61] Chen Y, Yang H, Luo Y. Parameter sensitivity analysis and configuration optimization of indirect evaporative cooler (IEC) considering condensation. Applied Energy. 2017;194:440-53.
[62] Liu Q, Guo C, Ma X, You Y, Li Y. Experimental study on total heat transfer efficiency evaluation of an indirect evaporative cooler. Applied Thermal Engineering. 2020;174.
[63] Guo C, Chen T, Zheng B, Liu Q, Lv J. Experimental study on evaluation index of indirect evaporative cooling heat transfer performance. Energy Procedia. 2019;158:5789-94.
[64] Pakari A, Ghani S. Regression models for performance prediction of counter flow dew point evaporative cooling systems. Energy Conversion and Management. 2019;185:562-73.
[65] Zhu G, Chen W, Lu S. Modelling of a dew-point effectiveness correlation for Maisotsenko cycle heat and mass exchanger. Chemical Engineering and Processing - Process Intensification. 2019;145.
[66] Adam A, Han D, He W, Chen J. Numerical analysis of cross-flow plate type indirect evaporative cooler: Modeling and parametric analysis. Applied Thermal Engineering. 2021;185.
[67] De Antonellis S, Joppolo CM, Liberati P, Milani S, Romano F. Modeling and experimental study of an indirect evaporative cooler. Energy and Buildings. 2017;142:147-57.
[68] De Antonellis S, Cignatta L, Facchini C, Liberati P. Effect of heat exchanger plates geometry on performance of an indirect evaporative cooling system. Applied Thermal Engineering. 2020;173.
[69] Khalid O, Ali M, Sheikh NA, Ali HM, Shehryar M. Experimental analysis of an improved Maisotsenko cycle design under low velocity conditions. Applied Thermal Engineering. 2016;95:288-95.
[70] Pandelidis D, Cichoń A, Pacak A, Anisimov S, Drąg P. Application of the cross-flow Maisotsenko cycle heat and mass exchanger to the moderate climate in different configurations in air-conditioning systems. Int J Heat Mass Transfer. 2018;122:806-17.
[71] Tariq R, Sheikh NA, Xamán J, Bassam A. Recovering waste energy in an indirect evaporative cooler – A case for combined space air conditioning for human occupants and produce commodities. Building and Environment. 2019;152:105-21.
[72] Anisimov S, Pandelidis D, Jedlikowski A. Performance study of the indirect evaporative air cooler and heat recovery exchanger in air conditioning system during the summer and winter operation. Energy. 2015;89:205-25.
[73] Tulsidasani TR, Sawhney RL, Singh SP, Sodha MS. Recent research on an indirect evaporative cooler (IEC) Part 1: optimization of the COP. International Journal of Energy Research. 1997;21(12):1099-108.
[74] Wang F, Sun T, Huang X, Chen Y, Yang H. Experimental research on a novel porous ceramic tube type indirect evaporative cooler. Applied Thermal Engineering. 2017;125:1191-9.
[75] Duan Z, Zhan C, Zhang X, Mustafa M, Zhao X, Alimohammadisagvand B, et al. Indirect evaporative cooling: Past, present and future potentials. Renewable and Sustainable Energy Reviews. 2012;16(9):6823-50.
[76] Zhang J, Dong X, Li Y, Sun S. A study on the performance of tube indirect evaporative cooling air conditioning unit Refrigeration and Air Conditioning. 2018;32(4):416-9.
[77] Sun T, Huang X, Chen Y, Zhang H. Experimental investigation of water spraying in an indirect evaporative cooler from nozzle type and spray strategy perspectives. Energy and Buildings. 2020;214.
[78] Chen Q, Burhan M, Shahzad MW, Ybyraiymkul D, Akhtar FH, Ng KC. Simultaneous production of cooling and freshwater by an integrated indirect evaporative cooling and humidification-dehumidification desalination cycle. Energy Convers Manage. 2020;221.
[79] Li W-Y, Li Y-C, Zeng L-y, Lu J. Comparative study of vertical and horizontal indirect evaporative cooling heat recovery exchangers. International Journal of Heat and Mass Transfer. 2018;124:1245-61.
[80] Pandelidis D, Niemierka E, Pacak A, Jadwiszczak P, Cichoń A, Drąg P, et al. Performance study of a novel dew point evaporative cooler in the climate of central Europe using building simulation tools. Building and Environment. 2020;181.
[81] Riffat SB, Zhu J. Mathematical model of indirect evaporative cooler using porous ceramic and heat pipe. Applied Thermal Engineering. 2004;24(4):457-70.

[82] Rajski K, Danielewicz J, Brychcy E. Performance Evaluation of a Gravity-Assisted Heat Pipe-Based Indirect Evaporative Cooler. Energies. 2020;13(1).
[83] Boukhanouf R, Amer O, Ibrahim H, Calautit J. Design and performance analysis of a regenerative evaporative cooler for cooling of buildings in arid climates. Building and Environment. 2018;142:1-10.
[84] Amer O. A heat pipe and porous ceramic based sub wet-bulb temperature evaporative cooler: a theoretical and experimental study: University of Nottingham; 2017.
[85] Park J-Y, Kim B-J, Yoon S-Y, Byon Y-S, Jeong J-W. Experimental analysis of dehumidification performance of an evaporative cooling-assisted internally cooled liquid desiccant dehumidifier. Applied Energy. 2019;235:177-85.
[86] Golizadeh Akhlaghi Y, Badiei A, Zhao X, Aslansefat K, Xiao X, Shittu S, et al. A constraint multi-objective evolutionary optimization of a state-of-the-art dew point cooler using digital twins. Energy Conversion and Management. 2020;211.
[87] Kabeel AE, Bassuoni MM, Abdelgaied M. Experimental study of a novel integrated system of indirect evaporative cooler with internal baffles and evaporative condenser. Energy Conversion and Management. 2017;138:518-25.
[88] Kabeel AE, Abdelgaied M, Sathyamurthy R, Arunkumar T. Performance improvement of a hybrid air conditioning system using the indirect evaporative cooler with internal baffles as a pre-cooling unit. Alexandria Engineering Journal. 2017;56(4):395-403.
[89] Kabeel AE, Abdelgaied M, Feddaoui MB. Hybrid system of an indirect evaporative air cooler and HDH desalination system assisted by solar energy for remote areas. Desalination. 2018;439:162-7.
[90] Ali M, Ahmad W, Sheikh NA, Ali H, Kousar R, Rashid Tu. Performance enhancement of a cross flow dew point indirect evaporative cooler with circular finned channel geometry. Journal of Building Engineering. 2021;35.
[91] Zheng B, Guo C, Chen T, Shi Q, Lv J, You Y. Development of an experimental validated model of cross-flow indirect evaporative cooler with condensation. Applied Energy. 2019;252.
[92] Liu Y, Li JM, Yang X, Zhao X. Two-dimensional numerical study of a heat and mass exchanger for a dew-point evaporative cooler. Energy. 2019;168:975-88.
[93] Lin J, Wang RZ, Kumja M, Bui TD, Chua KJ. Modelling and experimental investigation of the cross-flow dew point evaporative cooler with and without dehumidification. Applied Thermal Engineering. 2017;121:1-13.
[94] Liberati P, De Antonellis S, Leone C, Joppolo CM, Bawa Y. Indirect Evaporative cooling systems: Modelling and performance analysis. Energy Procedia. 2017;140:475-85.
[95] Zhou Y, Zhang T, Wang F, Yu Y. Performance analysis of a novel thermoelectric assisted indirect evaporative cooling system. Energy. 2018;162:299-308.
[96] Rogdakis ED, Koronaki IP, Tertipis DN. Experimental and computational evaluation of a Maisotsenko evaporative cooler at Greek climate. Energy and Buildings. 2014;70:497-506.
[97] Boukhanouf R, Alharbi A, Ibrahim HG, Amer O, Worall M. Computer modelling and experimental investigation of building integrated sub-wet bulb temperature evaporative cooling system. Applied Thermal Engineering. 2017;115:201-11.
[98] Chen Y, Yang H, Luo Y. Investigation on solar assisted liquid desiccant dehumidifier and evaporative cooling system for fresh air treatment. Energy. 2018;143:114-27.
[99] Zhao X, Liu S, Riffat SB. Comparative study of heat and mass exchanging materials for indirect evaporative cooling systems. Building and Environment. 2008;43(11):1902-11.
[100] Bolotin S, Vager B, Vasilijev V. Comparative analysis of the cross-flow indirect evaporative air coolers. International Journal of Heat and Mass Transfer. 2015;88:224-35.
[101] Meng D, Lv J, Chen Y, Li H, Ma X. Visualized experimental investigation on cross-flow indirect evaporative cooler with condensation. Applied Thermal Engineering. 2018;145:165-73.
[102] Guilizzoni M, Milani S, Liberati P, De Antonellis S. Effect of plates coating on performance of an indirect evaporative cooling system. International Journal of Refrigeration. 2019;104:367-75.
[103] Khandelwal A, Talukdar P, Jain S. Energy savings in a building using regenerative evaporative cooling. Energy and Buildings. 2011;43(2-3):581-91.
[104] Hutter C, Büchi D, Zuber V, Rudolf von Rohr P. Heat transfer in metal foams and designed porous media. Chemical Engineering Science. 2011;66(17):3806-14.
[105] Chen C-C, Huang P-C. Numerical study of heat transfer enhancement for a novel flat-plate solar water collector using metal-foam blocks. International Journal of Heat and Mass Transfer. 2012;55(23-24):6734-56.
[106] Rashidi S, Kashefi MH, Kim KC, Samimi-Abianeh O. Potentials of porous materials for energy management in heat exchangers – A comprehensive review. Applied Energy. 2019;243:206-32.
[107] Lee J, Lee D-Y. Experimental study of a counter flow regenerative evaporative cooler with finned channels. International Journal of Heat and Mass Transfer. 2013;65:173-9.
[108] Wang F, Liang C, Zhang X. Research of anti-frosting technology in refrigeration and air conditioning fields: A review. Renewable and Sustainable Energy Reviews. 2018;81:707-22.

[109] Zhuang D, Ding G, Hu H, Fujino H, Inoue S. Condensing droplet behaviors on fin surface under dehumidifying condition. Part II: Experimental validation. Applied Thermal Engineering. 2016;105:345-52.
[110] Min Y, Chen Y, Yang H. Investigation on dynamic behaviour of condensation heat transfer in indirective evaporative cooler. Indoor Built Environ. 2020:1420326X20944415.
[111] Zhan C, Zhao X, Smith S, Riffat SB. Numerical study of a M-cycle cross-flow heat exchanger for indirect evaporative cooling. Building and Environment. 2011;46(3):657-68.
[112] Zhan C, Duan Z, Zhao X, Smith S, Jin H, Riffat S. Comparative study of the performance of the M-cycle counter-flow and cross-flow heat exchangers for indirect evaporative cooling – Paving the path toward sustainable cooling of buildings. Energy. 2011;36(12):6790-805.
[113] Velasco Gómez E, Tejero González A, Rey Martínez FJ. Experimental characterisation of an indirect evaporative cooling prototype in two operating modes. Applied Energy. 2012;97:340-6.
[114] Ham S-W, Jeong J-W. DPHX (dew point evaporative heat exchanger): System design and performance analysis. Energy. 2016;101:132-45.
[115] Kim H-J, Ham S-W, Yoon D-S, Jeong J-W. Cooling performance measurement of two cross-flow indirect evaporative coolers in general and regenerative operation modes. Applied Energy. 2017;195:268-77.
[116] Al-Zubaydi AYT, Hong G. Experimental study of a novel water-spraying configuration in indirect evaporative cooling. Applied Thermal Engineering. 2019;151:283-93.
[117] Ramkumar R, Ragupathy A. Experimental investigation of indirect evaporative cooler using clay pipe. Journal of Thermal Engineering. 2017;3(2):1163-80.
[118] Kim N-H. Performance of an indirect evaporative cooler (IEC) made of PET/cellulose composite sheet as wetting media. Applied Thermal Engineering. 2021;186.
[119] Heidarinejad G, Moshari S. Novel modeling of an indirect evaporative cooling system with cross-flow configuration. Energy and Buildings. 2015;92:351-62.
[120] Shirmohammadi R, Gilani N. Effectiveness enhancement and performance evaluation of indirect-direct evaporative cooling system for a wide variety of climates. Environmental Progress & Sustainable Energy. 2018;38(3).
[121] Fikri B, Sofia E, Putra N. Experimental analysis of a multistage direct-indirect evaporative cooler using a straight heat pipe. Appl Therm Eng. 2020;171.
[122] Huang X, Lv W, Liu J, Li X. Application of evaporative cooling and mechanical refrigeration combined air conditioning unit to Baoji natatorium. Heating Ventilating & Air Conditioning. 2017;47(6):58-61.
[123] Huang X, Qu Y, Di Y. Application of multi-stage evaporative cooling air conditioning system to northwest China. Heating Ventilating & Air Conditioning. 2004;34(6):67-71.
[124] Li W, Shi W, Wang J, Li Y, Lu J. Experimental study of a novel household exhaust air heat pump enhanced by indirect evaporative cooling. Energy and Buildings. 2021.
[125] Gurubalan A, Maiya MP, Geoghegan PJ. A comprehensive review of liquid desiccant air conditioning system. Applied Energy. 2019;254.
[126] Delfani S, Esmaeelian J, Pasdarshahri H, Karami M. Energy saving potential of an indirect evaporative cooler as a pre-cooling unit for mechanical cooling systems in Iran. Energy and Buildings. 2010;42(11):2169-76.
[127] Min Y, Chen Y, Shi W, Yang H. Applicability of indirect evaporative cooler for energy recovery in hot and humid areas: Comparison with heat recovery wheel. Applied Energy. 2021;287.
[128] Cui, Sun, Zhang, Jin. On the Study of a Hybrid Indirect Evaporative Pre-Cooling System for Various Climates. Energies. 2019;12(23).
[129] Cui X, Chua KJ, Islam MR, Ng KC. Performance evaluation of an indirect pre-cooling evaporative heat exchanger operating in hot and humid climate. Energy Conversion and Management. 2015;102:140-50.
[130] Pandelidis D, Cichoń A, Pacak A, Anisimov S, Drąg P. Counter-flow indirect evaporative cooler for heat recovery in the temperate climate. Energy. 2018;165:877-94.
[131] Farmahini Farahani M, Heidarinejad G, Delfani S. A two-stage system of nocturnal radiative and indirect evaporative cooling for conditions in Tehran. Energy and Buildings. 2010;42(11):2131-8.
[132] Katramiz E, Al Jebaei H, Alotaibi S, Chakroun W, Ghaddar N, Ghali K. Sustainable cooling system for Kuwait hot climate combining diurnal radiative cooling and indirect evaporative cooling system. Energy. 2020;213.
[133] Kuzmic N, Law YLE, Dworkin SB. Numerical heat transfer comparison study of hybrid and non-hybrid ground source heat pump systems. Applied Energy. 2016;165:919-29.
[134] Luo J, Zhao H, Jia J, Xiang W, Rohn J, Blum P. Study on operation management of borehole heat exchangers for a large-scale hybrid ground source heat pump system in China. Energy. 2017;123:340-52.
[135] Menberg K, Heo Y, Choi W, Ooka R, Choudhary R, Shukuya M. Exergy analysis of a hybrid ground-source heat pump system. Applied Energy. 2017;204:31-46.
[136] Khalajzadeh V, Farmahini-Farahani M, Heidarinejad G. A novel integrated system of ground heat exchanger and indirect evaporative cooler. Energy and Buildings. 2012;49:604-10.

[137] Nemati N, Omidvar A, Rosti B. Performance evaluation of a novel hybrid cooling system combining indirect evaporative cooler and earth-air heat exchanger. Energy. 2021;215.
[138] Rafique MM, Gandhidasan P, Bahaidarah HMS. Liquid desiccant materials and dehumidifiers – A review. Renewable and Sustainable Energy Reviews. 2016;56:179-95.
[139] Vivekh P, Kumja M, Bui DT, Chua KJ. Recent developments in solid desiccant coated heat exchangers – A review. Applied Energy. 2018;229:778-803.
[140] Chen L, Tan Y. The performance of a desiccant wheel air conditioning system with high-temperature chilled water from natural cold source. Renewable Energy. 2020;146:2142-57.
[141] Cui X, Islam MR, Mohan B, Chua KJ. Theoretical analysis of a liquid desiccant based indirect evaporative cooling system. Energy. 2016;95:303-12.
[142] Sohani A, Sayyaadi H, Hasani Balyani H, Hoseinpoori S. A novel approach using predictive models for performance analysis of desiccant enhanced evaporative cooling systems. Applied Thermal Engineering. 2016;107:227-52.
[143] Lee S-J, Kim H-J, Dong H-W, Jeong J-W. Energy saving assessment of a desiccant-enhanced evaporative cooling system in variable air volume applications. Applied Thermal Engineering. 2017;117:94-108.
[144] Zhang F, Yin Y, Zhang X. Performance analysis of a novel liquid desiccant evaporative cooling fresh air conditioning system with solution recirculation. Building and Environment. 2017;117:218-29.
[145] Comino F, Ruiz de Adana M, Peci F. Energy saving potential of a hybrid HVAC system with a desiccant wheel activated at low temperatures and an indirect evaporative cooler in handling air in buildings with high latent loads. Applied Thermal Engineering. 2018;131:412-27.
[146] Bang J-I, Park J-Y, Jo Y-L, Jeong J-W, Choi A, Sung M. Sterilization effectiveness of in-duct ultraviolet germicidal irradiation system in liquid desiccant and indirect/direct evaporative cooling-assisted 100% outdoor air system. Building and Environment. 2020;186.
[147] Goldsworthy M, White S. Optimisation of a desiccant cooling system design with indirect evaporative cooler. International Journal of Refrigeration. 2011;34(1):148-58.
[148] Buker MS, Riffat SB. Performance Analysis of a Combined Building Integrated PV/T Collector with a Liquid Desiccant Enhanced Dew Point Cooler. Energy Procedia. 2016;91:717-27.
[149] Saghafifar M, Gadalla M. Performance assessment of integrated PV/T and solid desiccant air-conditioning systems for cooling buildings using Maisotsenko cooling cycle. Solar Energy. 2016;127:79-95.
[150] Fang K, Qiang T, Xuan Y. Study on coupling air conditioning system of solar refrigeration and dew point evaporative cooling. Journal of Xi'an Polytechnic University. 2020;34(2):52-9.
[151] Li R, Li F, Han R. Solar ejector and indirect evaporative coupled cooling system performance analysis based on Lanzhou region. Journal of Huaqiao University (Natural Science). 2018;39(4):577-82.
[152] De Antonellis S, Joppolo CM, Liberati P. Performance measurement of a cross-flow indirect evaporative cooler: Effect of water nozzles and airflows arrangement. Energy and Buildings. 2019;184:114-21.
[153] Huang X. Principle and Equipment of Evaporative Cooling Air Conditioning. first ed. China: China Machine Press; 2019.
[154] Lacour SOL, Trinquet F, Vendee PE, Vallet A, Delahaye A, Fournaison L. Assessment of the wet area of a heat exchanger exposed to a water spray. Applied Thermal Engineering. 2018;128:434-43.
[155] Montazeri H, Blocken B, Hensen JLM. Evaporative cooling by water spray systems: CFD simulation, experimental validation and sensitivity analysis. Building and Environment. 2015;83:129-41.
[156] Hu M, Xiao F, Jørgensen JB, Wang S. Frequency control of air conditioners in response to real-time dynamic electricity prices in smart grids. Applied Energy. 2019;242:92-106.
[157] Yang S, Wan MP, Ng BF, Dubey S, Henze GP, Chen W, et al. Experimental study of model predictive control for an air-conditioning system with dedicated outdoor air system. Applied Energy. 2020;257.
[158] Wang S, Tang R. Supply-based feedback control strategy of air-conditioning systems for direct load control of buildings responding to urgent requests of smart grids. Applied Energy. 2017;201:419-32.
[159] Zhuang C, Wang S. Risk-based online robust optimal control of air-conditioning systems for buildings requiring strict humidity control considering measurement uncertainties. Applied Energy. 2020;261.
[160] Wang J, Chen X, Xie J, Xu S, Yu K, Gan L. Dynamic control strategy of residential air conditionings considering environmental and behavioral uncertainties. Applied Energy. 2019;250:1312-20.
[161] Jiang Y, Wang X, Zhao H, Wang L, Yin X, Jia L. Dynamic modeling and economic model predictive control of a liquid desiccant air conditioning. Applied Energy. 2020;259.
[162] Zhuang C, Wang S, Tang R. Optimal Design of Multi-zone Air-conditioning Systems for Buildings Requiring Strict Humidity Control. Energy Procedia. 2019;158:3202-7.
[163] Chen Y, Yan H, Yang H. Comparative study of on-off control and novel high-low control of regenerative indirect evaporative cooler (RIEC). Applied Energy. 2018;225:233-43.
[164] Yan H, Chen Y, Zhang W. Year-round-based optimization of high-low control in the regenerative indirect evaporative cooler (RIEC). Science and Technology for the Built Environment. 2019;25(10):1394-405.

[165] Sohani A, Sayyaadi H, Zeraatpisheh M. Optimization strategy by a general approach to enhance improving potential of dew-point evaporative coolers. Energy Conversion and Management. 2019;188:177-213.
[166] Qi R, Lu L, Yang H, Qin F. Investigation on wetted area and film thickness for falling film liquid desiccant regeneration system. Applied Energy. 2013;112:93-101.
[167] Zhang F, Zhang Z, Geng J. Study on shrinkage characteristics of heated falling liquid films. AIChE Journal. 2005;51(11):2899-907.